Genomic diversity and global distribution of *Saccharomyces eubayanus,* the wild ancestor of hybrid lager-brewing yeasts

Quinn K. Langdon[1], David Peris[1,2,3], Juan I. Eizaguirre[4], Dana A. Opulente[1,2], Kelly V. Buh[1], Kayla Sylvester[1,2], Martin Jarzyna[1,2], María E. Rodríguez[5], Christian A. Lopes[5], Diego Libkind[4,@], Chris Todd Hittinger[1,2,@]

[1]Laboratory of Genetics, J. F. Crow Institute for the Study of Evolution, Wisconsin Energy Institute, Genome Center of Wisconsin, University of Wisconsin-Madison, Madison, WI 53706, USA

[2]DOE Great Lakes Bioenergy Research Center, University of Wisconsin-Madison, Madison, WI 53706, USA

[3]Department of Food Biotechnology, Institute of Agrochemistry and Food Technology (IATA), CSIC, Valencia, Spain

[4]Laboratorio de Microbiología Aplicada, Biotecnología y Bioinformática de Levaduras, Instituto Andino Patagónico de Tecnologías Biológicas y Geoambientales (IPATEC), Consejo Nacional de Investigaciones, Científicas y Técnicas (CONICET)-Universidad Nacional del Comahue, 8400 Bariloche, Argentina

[5]Instituto de Investigación y Desarrollo en Ingeniería de Procesos, Biotecnología y Energías Alternativas (PROBIEN, CONICET-UNCo), Neuquén, Argentina

[@]Corresponding authors: CTH cthittinger@wisc.edu & DL diego.libkind@gmail.com

Abstract:

S. eubayanus, the wild, cold-tolerant parent of hybrid lager-brewing yeasts, has a complex and understudied natural history. The exploration of this diversity can be used both to develop new brewing applications and to enlighten our understanding of the dynamics of yeast evolution in the wild. Here, we integrate whole genome sequence and phenotypic data of 200 *S. eubayanus* strains, the largest collection to date. *S. eubayanus* has a multilayered population structure, consisting of two major populations that are further structured into six subpopulations. Four of these subpopulations are found exclusively in the Patagonian region of South America; one is found predominantly in Patagonia and sparsely in Oceania and North America; and one is specific to the Holarctic ecozone. *S. eubayanus* is most abundant and genetically diverse in Patagonia, where some locations harbor more genetic diversity than is found outside of South America. All but one subpopulation shows isolation-by-distance, and gene flow between subpopulations is low. However, there are strong signals of ancient and recent outcrossing, including two admixed lineages, one that is sympatric with and one that is mostly isolated from its parental populations. Despite *S. eubayanus*' extensive genetic diversity, it has relatively little phenotypic diversity, and all subpopulations performed similarly under most conditions tested. Using our extensive biogeographical data, we constructed a robust model that predicted all known and a handful of additional regions of the globe that are climatically suitable for *S. eubayanus*, including Europe. We conclude that this industrially relevant species has rich wild diversity with many factors contributing to its complex distribution and biology.

47 Introduction:

48 In microbial population genomics, the interplay of human association and natural
49 variation is still poorly understood. The genus *Saccharomyces* is an optimal model to address
50 these questions for eukaryotic microbes, as it contains both partly human-associated species (i.e.
51 *Saccharomyces cerevisiae*) and mostly wild species (e.g. *Saccharomyces paradoxus)*. These two
52 examples also illustrate the complexity of studying yeast population genomics. Much of *S.*
53 *cerevisiae* population structure is admixed, and several lineages show signatures of
54 domestication (Liti et al. 2009; Schacherer et al. 2009; Gallone et al. 2016; Gonçalves et al.
55 2016). In contrast, *S. paradoxus* is almost exclusively found in the wild and has a population
56 structure that is correlated with geography (Leducq et al. 2014; Eberlein et al. 2019). Pure
57 isolates of their more distant relative *Saccharomyces eubayanus* have only ever been isolated
58 from wild environments; yet, hybridizations between *S. cerevisiae* and *S. eubayanus* were key
59 innovations that enabled cold fermentation and lager brewing (Libkind et al. 2011; Gibson and
60 Liti 2015; Hittinger et al. 2018; Baker et al. 2019). Other hybrids with contributions from *S.*
61 *eubayanus* have been isolated from industrial environments (Almeida et al. 2014; Nguyen and
62 Boekhout 2017), indicating that this species has long been playing a role in shaping many
63 fermented products. This association with both natural and domesticated environments makes *S.*
64 *eubayanus* an excellent model where both wild diversity and domestication can be investigated.
65 Since the discovery of *S. eubayanus* in Patagonia (Libkind et al. 2011), this species has
66 received much attention, both for brewing applications and understanding the evolution, ecology,
67 population genomics of the genus *Saccharomyces* (Sampaio 2018). In the years since its
68 discovery, many new globally distributed isolates have been found (Bing et al. 2014; Peris et al.
69 2014; Rodríguez et al. 2014; Gayevskiy and Goddard 2016; Peris et al. 2016; Eizaguirre et al.

2018). Prior research has suggested that *S. eubayanus* is most abundant and diverse in the Patagonian region of South America, where there are two major populations (Patagonia A/Population A/PA and Patagonia B/Population B/PB) that recent multilocus data suggested are further divided into five subpopulations (PA-1, PA-2, PB-1, PB-2, and PB-3) (Eizaguirre et al. 2018). There are two early-diverging lineages, West China and Sichuan, which were identified through multilocus data (Bing et al. 2014) and whose sequence divergences relative to other strains of *S. eubayanus* are nearly that of currently recognized species boundaries (Peris et al. 2016; Sampaio and Gonçalves 2017; Naseeb et al. 2018). A unique admixed lineage has been found only in North America, which has approximately equal contributions from PA and PB (Peris et al. 2014, 2016). Other isolates from outside Patagonia belong to PB, either the PB-1 subpopulation that is also found in Patagonia (Gayevskiy and Goddard 2016; Peris et al. 2016), or a Holarctic-specific subpopulation that includes isolates from Tibet and from North Carolina, USA (Bing et al. 2014; Peris et al. 2016). This Holarctic subpopulation includes the closest known wild relatives of the *S. eubayanus* subgenomes of lager-brewing yeasts (Bing et al. 2014; Peris et al. 2016).

To explore the geographic distribution, ecological niche, and genomic diversity of this industrially relevant species, here, we present an analysis of whole genome sequencing data for 200 *S. eubayanus* strains. This dataset confirms the previously proposed population structure (Peris et al. 2014, 2016; Eizaguirre et al. 2018) and extends the analysis to fully explore genomic diversity. Even though *S. eubayanus* is genetically diverse and globally distributed, there are not large phenotypic differences between subpopulations. This genomic dataset includes evidence of gene flow and admixture in sympatry, as well as admixture in parapatry or allopatry. While *S. eubayanus* has a well-differentiated population structure, isolation by distance occurs within

subpopulations that are found globally, as well as within subpopulations restricted to a handful of locations. Much of the genetic diversity is limited to northern Patagonia, but modeling suggests that there are more geographic areas that are climatically suitable for this species, including Europe. *S. eubayanus* maintains genetic diversity over several dimensions, including multiple high-diversity sympatric populations and a low-diversity widespread invasive lineage. The diversity and dispersal of this eukaryotic microbial species mirror observations in plants and animals, including humans, which shows how biogeographical and evolutionary forces can be shared across organismal sizes, big and small.

Results:

Global and regional *S. eubayanus* population structure and ecology:

To expand on existing data (Libkind et al. 2011; Bing et al. 2014; Peris et al. 2014; Rodríguez et al. 2014; Gayevskiy and Goddard 2016; Peris et al. 2016; Eizaguirre et al. 2018), we sequenced the genomes of 174 additional strains of *S. eubayanus*, bringing our survey to 200 *S. eubayanus* genomes. This large collection provides the most comprehensive dataset to date for *S. eubayanus*. We note that the dataset does not contain West China or Sichuan strains (Bing et al. 2014), which were unavailable for study and may constitute a distinct species or subspecies. These strains were globally distributed (Figure 1A), but the majority of our strains were from South America (172 total, 155 newly sequenced here). The next most abundant continent was North America with 26 strains (19 new to this publication). We also analyzed whole genome sequence data for the single strain from New Zealand (Gayevskiy and Goddard 2016) and the single Tibetan isolate with available whole genome sequence data (Bing et al. 2014; Brouwers et al. 2019). The collection sites in South America span from northern Patagonia to Tierra del

116 Fuego (Figure 1B), while the North American isolates have been sparsely found throughout the
117 continent, including the Canadian province of New Brunswick and the American states of
118 Washington, Wisconsin, North Carolina, and South Carolina (Figure 1C).
119

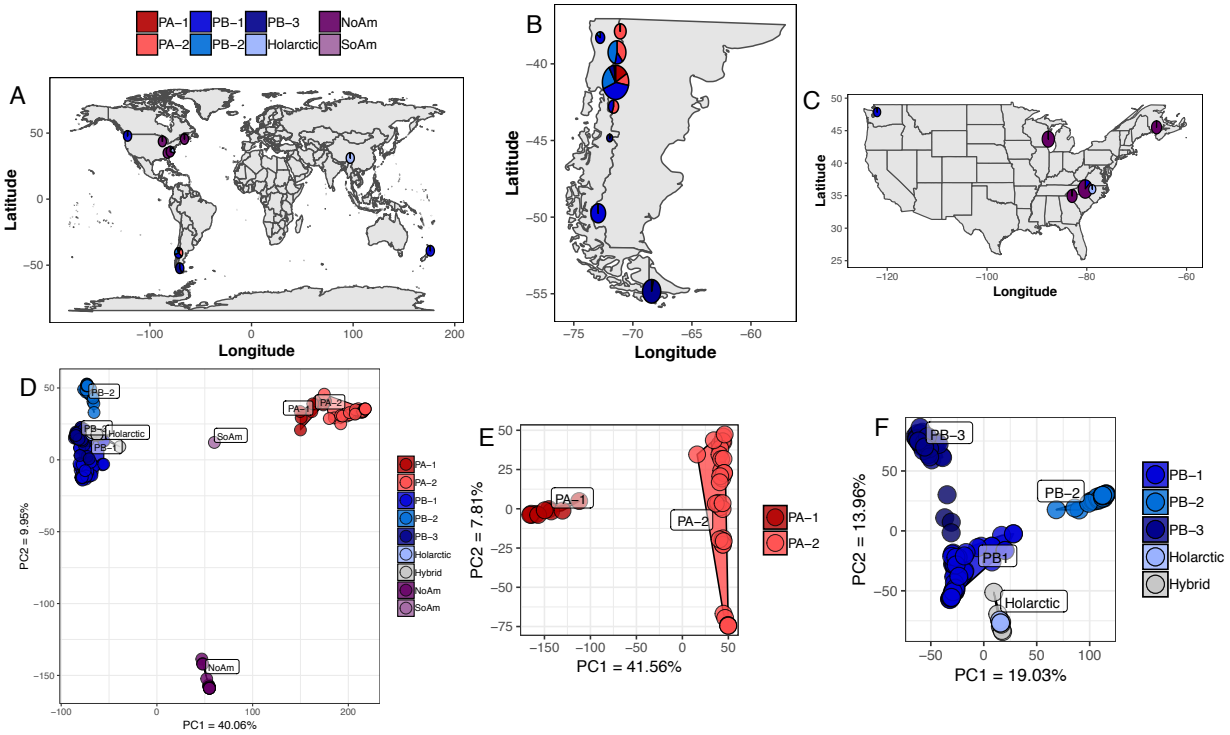

120 **Figure 1.** *S. eubayanus* distribution and population structure.
121 *S. eubayanus* has a global distribution and two major populations with six subpopulations. (A) Isolation
122 locations of *S. eubayanus* strains included in the dataset. For visibility, circle size is not scaled by the
123 number of strains. Subpopulation abundance is shown as pie charts. The Patagonian sampling sites have
124 been collapsed to two locations for clarity. Details of sites and subpopulations found in South America
125 (B) and North America (C) with circle size scaled by the number of strains. (D) Whole genome PCA of *S.*
126 *eubayanus* strains and five hybrids with large contributions from *S. eubayanus*. (E) PCA of just PA. (F)
127 PCA of just PB and hybrid *S. eubayanus* sub-genomes. Color legends in A and D apply to this and all
128 other figures.
129
130 To determine population structure, we took several approaches, including Principal
131 Component Analysis (PCA) (Jombart 2008), phylogenomic networks (Huson and Bryant 2006),
132 and STRUCTURE-like analyses (Lawson et al. 2012; Raj et al. 2014). All methods showed that
133 *S. eubayanus* has two large populations that can be further subdivided into a total of six non-

admixed subpopulations and one abundant North American admixed lineage (Figure 1D and Figure S1). We previously described the two major populations, PA and PB-Holarctic (Peris et al. 2014, 2016), as well as the subpopulations PA-1, PA-2, PB-1, PB-2, Holarctic, and the North American admixed lineage (Peris et al. 2016). PB-3 had been suggested by multilocus data (Eizaguirre et al. 2018), and our new analyses confirm this subpopulation with whole genome sequence data. All of the strains isolated from outside of South America belonged to either the previously described North American admixed lineage (NoAm) or one of two PB subpopulations, PB-1 or Holarctic. This dataset included novel PB-1 isolates from the states of Washington (yHRMV83) and North Carolina (yHKB35). Unexpectedly, from this same site in North Carolina, we also obtained new isolates of the NoAm admixed lineage (Figure 1C and Table S1), and we obtained additional new NoAm strains in South Carolina. Together, with the North Carolina strains reported here and previously (Peris et al. 2016), this region near the Blue Ridge Mountains harbors three subpopulations or lineages, PB-1, Holarctic, and NoAm. We were also successful in re-isolating the NoAm lineage from the same Wisconsin site, sampling two years later than what was first reported (Peris et al. 2014) (Table S1), indicating that the NoAm admixed lineage is established, not ephemeral, in this location. Additionally, we found one novel South American strain that was admixed between PA (~45%) and PB (~55%) (Figure 1D "SoAm"). This global distribution and the well-differentiated population structure of *S. eubayanus* is similar to what has been observed in *S. paradoxus* (Leducq et al. 2014, 2016) and *Saccharomyces uvarum* (Almeida et al. 2014).

S. eubayanus has been isolated from numerous substrates and hosts, and our large dataset afforded us the power to analyze host and substrate association by subpopulation. We found that PA-2 was associated with the seeds of *Araucaria araucana* (45.71% of isolates, p-val = 6.11E-

157 07, F-statistic = 15.29). Interestingly, while PB-1 was the most frequently isolated subpopulation
158 (34% of isolates), it has never been isolated from *A. araucana* seeds. Instead, PB-1 was
159 associated with *Nothofagus antarctica* (52.31% of isolates, p-val = 0.017, F-statistic = 3.10). PB-
160 1 was also the subpopulation isolated the most from *Nothofagus dombeyi* (75% of isolates from
161 this tree species), which is a common host of *S. uvarum* (Libkind et al. 2011; Eizaguirre et al.
162 2018). PB-2 was positively associated with *Nothofagus pumilio* (36.59% of isolates, p-val = 9.60
163 E-04, F-statistic = 6.59), which could be an ecological factor keeping PB-2 partly isolated from
164 its sympatric subpopulations, PA-2 and PB-1 (Figure 1C). PB-3 was associated with the fungal
165 parasite *Cyttaria darwinii* (14.29% of isolates, p-val = 0.039, F-statistic = 25.34) and
166 *Nothofagus betuloides* (28.57% of isolates, p-val = 5.02E-06, F-statistic = 60.35), which is only
167 found in southern Patagonia and is vicariant with *N. dombeyi*, a host of PB-1. PB-3 was
168 frequently isolated in southern Patagonia (49% of southern isolates) (Eizaguirre et al. 2018), and
169 its association with a southern-distributed tree species could play a role in its geographic range
170 and genetic isolation from the northern subpopulations. Neither *Nothofagus* nor *A. araucana* are
171 native to North America, and we found that our North American isolates were from multiple
172 diverse plant hosts, including *Juniperus virginiana*, *Diospyros virginiana, Cedrus* sp., and *Pinus*
173 sp. (Table S1), as well as from both soil and bark samples. In Patagonia, *S. eubayanus* has been
174 isolated from exotic *Quercus* trees (Eizaguirre et al. 2018), so even though *Nothofagus* and *A.*
175 *araucana* are common hosts, *S. eubayanus* can be found on a variety of hosts and substrates.
176 These observed differences in host and substrate could be playing a role in the maintenance of its
177 population structure, especially in sympatric regions of Patagonia.
178
179 All subpopulations grow at freezing temperatures and on diverse carbon sources:

S. eubayanus comes from a wide range of environments, so we tested if there were phenotypic differences between these subpopulations. We measured growth rates on several carbon sources and stress responses for a large subset of these strains (190) and 26 lager-brewing strains (Figure 2 and Figure S2). Lager-brewing strains grew faster on maltotriose than all subpopulations (p-val < 0.05, Figure 2A), which is consistent with this sugar being one of the most abundant in brewing wort but rare in nature (Salema-Oom et al. 2005). The Holarctic subpopulation grew slower on glucose and maltose compared to all other subpopulations (p-val < 0.05, Figure 2A, Table S2). Overall, the admixed NoAm lineage performed better than PB-1 (p-val = 0.038, Figure 2A), but there was no interaction with carbon source. Therefore, the admixed lineage's robustness in many conditions could play a role in its success in far-flung North American sites where no pure PA or PB strains have ever been found.

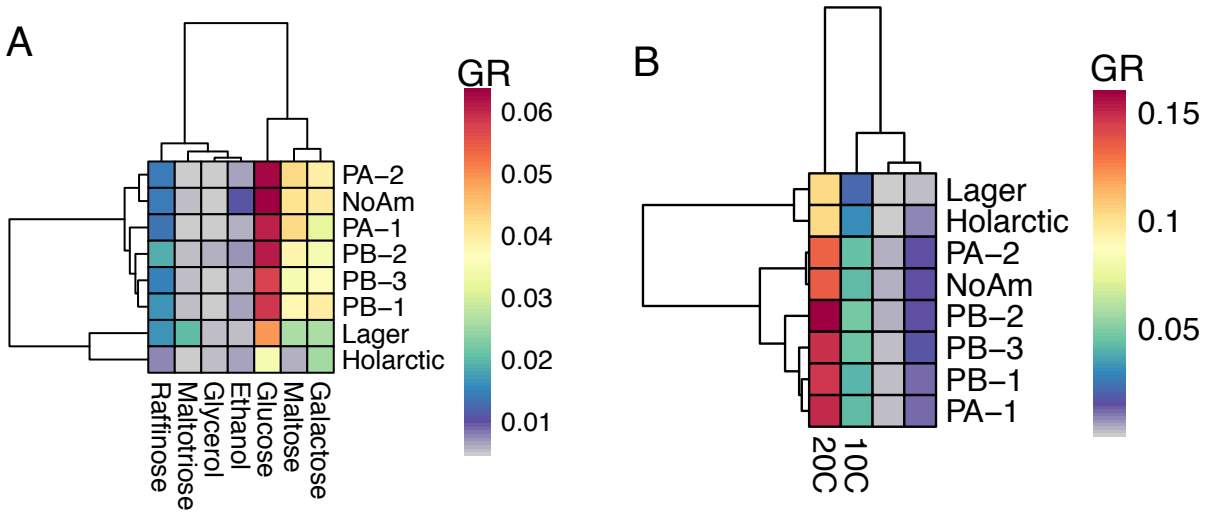

Figure 2. Phenotypic differences.
(A) Heat map of mean of maximum growth rate (change in OD/hour) (GR) on different carbon sources by subpopulation. Warmer colors designate faster growth. (B) Heat map of $\log_{10}$ normalized growth at different temperatures by subpopulation.

Since *S. eubayanus*' contribution to the cold-adaptation of hybrid brewing strains is well established (Libkind et al. 2011; Gibson et al. 2013; Baker et al. 2019), we measured growth at 0°C, 4°C, 10°C, and 20°C. All subpopulations grew at temperatures as low as 0°C (Figure 2B

and Figure S2), and all *S. eubayanus* subpopulations outperformed lager-brewing yeasts ($p < 0.05$). Within pure *S. eubayanus*, there were no temperature by subpopulation interactions, indicating that no subpopulation is more cryotolerant than any other subpopulation. In summary, we found that all strains that we tested grew similarly in many environments, and despite the large amount of genotypic diversity observed for this species, we observed much less phenotypic diversity (Figure 2).

Subpopulations are well differentiated:

The mating strategies and life cycle of *Saccharomyces*, with intratetrad mating and haploselfing, often lead to homozygous diploid individuals (Hittinger 2013). Nonetheless, in *S. cerevisiae*, many industrial strains are highly heterozygous (Gallone et al. 2016; Gonçalves et al. 2016; Peter et al. 2018). Here, we analyzed genome-wide heterozygosity in our collection of 200 strains and found only one individual with more than 20,000 heterozygous SNPs (Figure S3). When we phased highly heterozygous regions of its genome and analyzed the two phases separately, we found that both phases grouped within PB-1 (Figure S3C). Thus, while this strain is highly heterozygous, it has contributions from only one subpopulation.

This large collection of strains is a powerful resource to explore natural variation and population demography in a wild microbe, so we analyzed several common population genomic statistics in 50-kbp windows across the genome. We found that diversity was similar between subpopulations (Figure S4A). We also calculated Tajima's D and found that the genome-wide mean was zero or negative for each subpopulation (Figure S4B), which could be indicative of population expansions. In particular, the most numerous and widespread subpopulation, PB-1,

had the most negative and consistent Tajima's D, suggesting a recent population expansion is especially likely in this case.

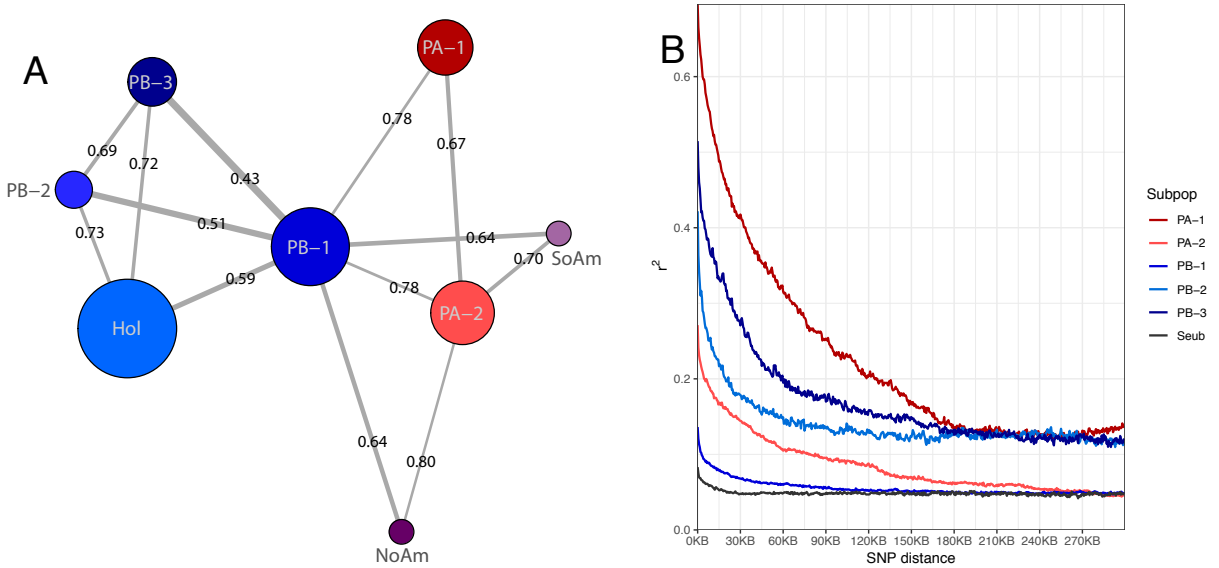

Figure 3. Population genomic parameters.
(A) Network built with pairwise F_{ST} values < 0.8 between each subpopulation. F_{ST} values are printed and correspond to line thickness, where lower values are thicker. Circle sizes correspond to genetic diversity.
(B) LD decay for each subpopulation (colors) and the species in whole (black).

For the non-admixed lineages, genome-wide average F_{ST} was consistently high across the genome (Figure S4C). In pairwise comparisons of F_{ST}, PB-1 had the lowest values of any subpopulation (Figure 3A, Figure S4D). These pairwise comparisons also showed that, within each population, there has been some gene flow between subpopulations, even though the subpopulations were generally well differentiated. Linkage disequilibrium (LD) decay indicated low recombination in these wild subpopulations (Figure 3B), with variability between subpopulations. For the species as a whole, LD decayed to one-half at about 5 kbp, which is somewhat higher than the 500bp - 3kbp observed in *S. cerevisiae* (Liti et al. 2009; Schacherer et al. 2009; Peter et al. 2018) and lower than the 9 kbp observed in *S. paradoxus* (Liti et al. 2009), indicating that there is less mating, outcrossing, and/or recombination in this wild species than *S. cerevisiae* and more than in *S. paradoxus*.

241

242 Recent admixture and historical gene flow between populations:

243 We previously reported the existence of 7 strains of an admixed lineage in Wisconsin,
244 USA, and New Brunswick, Canada (Peris et al. 2014, 2016). Here, we present 14 additional
245 isolates of this same admixed lineage. These new isolates were from the same site in Wisconsin,
246 as well as two new locations in North Carolina and South Carolina (Table S1). Strikingly, all 21
247 strains shared the exact same genome-wide ancestry profile (Figure 4A), indicating that they all
248 descended from the same outcrossing event between the two main populations of *S. eubayanus*.
249 These admixed strains were differentiated by 571 SNPs, which also delineated these strains
250 geographically (Figure 4B). Pairwise diversity and F_{ST} comparisons across the genomes suggest
251 that the PA parent came from the PA-2 subpopulation (Figure 4C and Figure S5A) and that the
252 PB parent was from the PB-1 subpopulation (Figure 4D and Figure S5A).

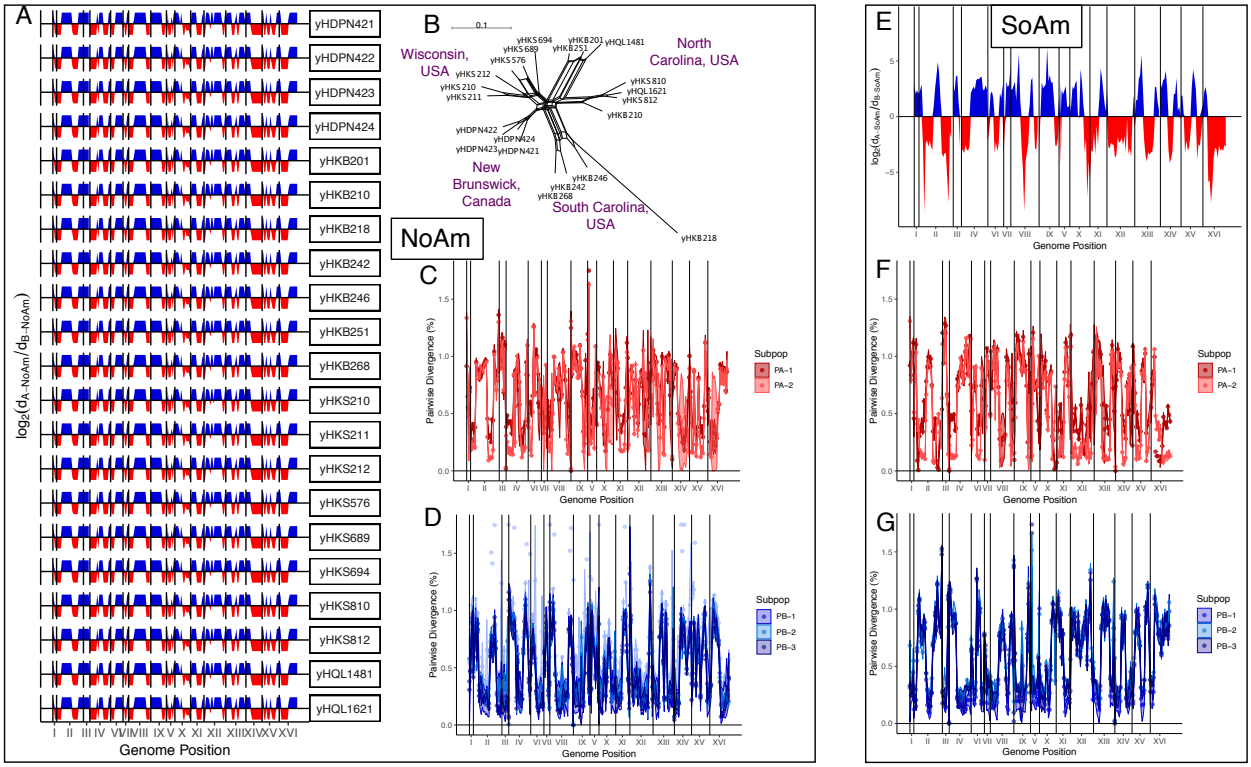

253
254 **Figure 4.** Genomic ancestries of NoAm and SoAm admixed lineages.

(A) For all 21 NoAm admixed strains, $\log_2$ ratio of the minimum PB-NoAm pairwise nucleotide sequence divergence (dB-NoAm) and the minimum PA-NoAm pairwise nucleotide sequence divergence (dA-NoAm) in 50-kbp windows. Colors and $\log_2 < 0$ or > 0 indicate that part of the genome is more closely related to PA or PB, respectively. (B) Neighbor-Net phylogenetic network reconstructed with the 571 SNPs that differentiate the NoAm strains. The scale bar represents the number of substitutions per site. Collection location is noted. (C) Pairwise nucleotide sequence divergence of the NoAm strain yHKS210 compared to strains from the PA-1 and PA-2 subpopulations of PA in 50-kbp windows. (D) Pairwise nucleotide sequence divergence of the NoAm strain yHKS210 compared to strains from the PB-1, PB-2, and PB-3 subpopulations of PB in 50-kbp windows. (E) $\log_2$ ratio of the minimum PB-SoAm pairwise nucleotide sequence divergence (dB-SoAm) and the minimum PA-SoAm pairwise nucleotide sequence divergence (dA-SoAm) in 50-kbp windows. Colors and $\log_2 < 0$ or > 0 indicate that part of the genome is more closely related to PA or PB, respectively. (F) Pairwise nucleotide sequence divergence of the SoAm strain compared to strains from the PA-1 and PA-2 subpopulations of PA in 50-kbp windows. (G) Pairwise nucleotide sequence divergence of the SoAm strain compared to strains of the PB-1, PB-2, and PB-3 subpopulations of PB in 50-kbp windows.

Here, we report a second instance of recent outcrossing between PA and PB. One other strain with fairly equal contributions from the two major populations, PA (~45%) and PB (~55%) (Figure 4E), was isolated from the eastern side of Nahuel Huapi National Park, an area that is sympatric for all subpopulations found in South America. This strain had a complex ancestry, where both PA-1 and PA-2 contributed to the PA portions of its genome (Figure 4F and Figure S5B), indicating that its PA parent was already admixed between PA-1 and PA-2. As with the NoAm admixed strains, the PB parent was from the PB-1 subpopulation (Figure 4G and Figure S5B). Together, these two admixed lineages show that outcrossing occurs between the two major populations, and that admixture and gene flow are likely ongoing within sympatric regions of South America.

We also found examples of smaller tracts of admixture between PA and PB that were detectable as 2-12% contributions. These introgressed strains included the taxonomic type strain of *S. eubayanus* (CBS12357^T), whose genome sequence was mostly inferred to be from PB-1, but it had a ~4% contribution from PA-1 (Figure S6). We found several other examples of admixture between PA and PB, as well as admixture between subpopulations of PA or of PB (Table S3). Notably, the PB contributions were usually from PB-1, the subpopulation with the

largest range, most hosts, and strongest signature of population expansion, factors that would tend to make contact with other subpopulations more likely.

In our collection of 200 strains, we observed nuclear genome contributions from *S. uvarum* in four strains. These four strains all shared the same introgression of ~150-kbp on chromosome XIV (Figure S7A&B). When we analyzed the portion of the genome contributed by *S. eubayanus*, we found that these strains were all embedded in the PB-1 subpopulation (Figure S7C). Analysis of the 150-kbp region from *S. uvarum* indicated that the closest *S. uvarum* population related to these introgressed strains was SA-B (Figure S7D), a population restricted to South America that has not previously been found to contribute to any known interspecies hybrids (Almeida et al. 2014). These strains thus represent an independent hybridization event between South American lineages of these two sister species that is not related to any known hybridization events among industrial strains (Almeida et al. 2014). These strains show that *S. eubayanus* and *S. uvarum* can and do hybridize in the wild, but the limited number (n=4) of introgressed strains, small introgression size (150-kbp), and shared breakpoints suggest that the persistence of hybrids in the wild is rare.

Northern Patagonia is a diversity hot spot:

Patagonia harbors the most genetic diversity of *S. eubayanus* in our dataset, and four subpopulations were found only there: PA-1, PA-2, PB-2, and PB-3 (Figure 1A and 4A). Therefore, we examined the genetic diversity and range distributions of the isolates from South America more closely. Nahuel Huapi National Park yielded isolates from all five subpopulations found in South America, was the only place where PA-1 was found, and was the location where the SoAm admixed strain was isolated (Figure 5A & B). All five sub-populations were found

north of 43°S, an important boundary during the last glaciation period that affects many organisms (Mathiasen and Premoli 2010; Premoli et al. 2010; Quiroga and Premoli 2010). Species-wide, there was more genetic diversity north of this boundary (Figure 5B). In contrast, only PB-1 and PB-3 were found south of 43°S, with both distributions reaching Tierra del Fuego. The southernmost strains were primarily PB-3 (89.7%), but they included two highly admixed PB-1 × PB-3 strains (Table S1 & S3).

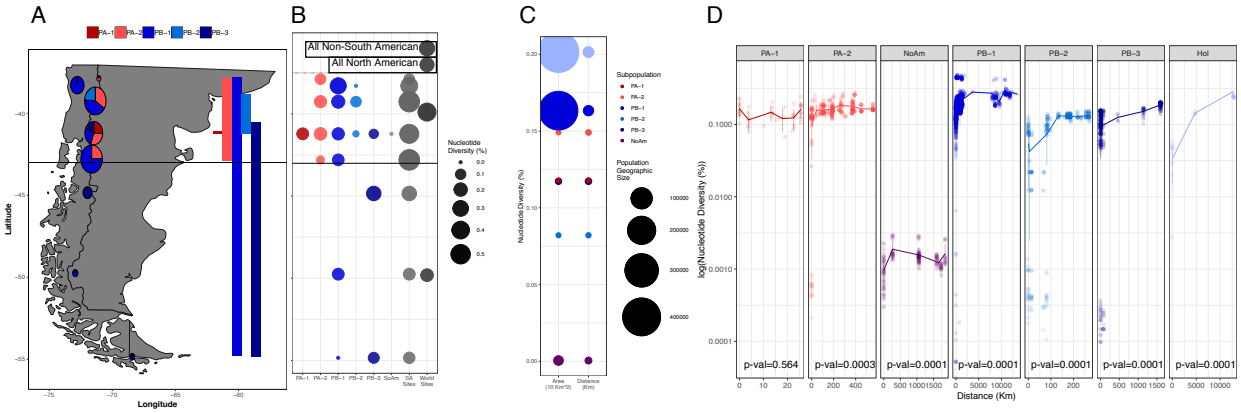

Figure 5. South American genomic diversity versus range, diversity by area, and isolation by distance. (A) Range and genomic diversity of South American sampling sites. Circle sizes correspond to nucleotide diversity of all strains from that site, and pie proportions correspond to each subpopulation's contribution to π at each site. Latitudinal range of each subpopulation is shown to the right. (B) Nucleotide diversity by subpopulation by sampling site, where larger and darker circles indicate more diversity. "SA Sites" in gray show the diversity of all strains found in each South American (SA) site. "World Sites" in darker gray show the nucleotide diversity of all North American or non-South American strains, regardless of subpopulation, compared to South American strains south or north of 43°S, aligned to mean latitude of all strains included in the analysis. (C) Correlation of nucleotide diversity and the area or distance a subpopulation covers. The y-axis shows the nucleotide diversity of each subpopulation, and circle sizes correspond to the geographic sizes of the subpopulations on a log10 scale. Note that PA-1 (dark red) is as diverse as PB-3 (dark blue) but encompasses a smaller area. (D) $\log_{10}$(pairwise nucleotide diversity) correlated with distance between strains, which demonstrates isolation by distance. Note that y-axes are all scaled the same but not the x-axes. Holarctic includes the *S. eubayanus* sub-genome of two lager-brewing strains. Figure S8A shows the individual plots for the NoAm lineage. Figure S8B shows the individual plot of PB-1.

Despite the limited geographic range of some subpopulations, their genetic diversity was high, and this diversity often did not scale with the geographic area over which they were found (Figure 5C). The widespread distribution of some subpopulations led us to question if there was isolation by distance within a subpopulation (Figure 5D). We used pairwise measures of

338 diversity and geographic distance between each strain and conducted Mantel tests for each
339 subpopulation. All subpopulations showed significant isolation by distance (Table S4), except
340 PA-1, likely because it had the smallest geographic range (25 km). Even the Mantel test for the
341 least diverse lineage, NoAm, was highly significant (p-val = 0.0001, R^2= 0.106), indicating that
342 each location has been evolving independently after their recent shared outcrossing and dispersal
343 event. Through these pairwise analyses, we also detected two strains from Cerro Ñielol, Chile,
344 that were unusually genetically divergent from the rest of PB-1 and could potentially be a novel
345 lineage (Figure S8).
346
347 Additional global regions are climatically suitable:
348 The sparse but global distribution of *S. eubayanus* raises questions about whether other
349 areas of the world could be suitable for this species. We used the maxent environmental niche
350 modeling algorithm implemented in Wallace (Kass et al. 2018) to model the global climatic
351 suitability for *S. eubayanus*, using GPS coordinates of all known *S. eubayanus* strains published
352 here and estimates of coordinates for the East Asian isolates (Bing et al. 2014). These niche
353 models were built using the WorldClim Bioclims, which are based on monthly temperature and
354 rainfall measures, reflecting both annual and seasonal trends, as well as extremes, such as the
355 hottest and coldest quarters. How climatic variables affect yeast distributions is an understudied
356 area, and building these models allowed us a novel way to explore climatic suitability.
357 Using all known locations of isolation (Figure 6), we found that the best model
358 (AIC=2122.4) accurately delineated the known distribution along the Patagonian Andes. In
359 North America, the strains from the Olympic Mountains of Washington state and the Blue Ridge
360 region of North Carolina fell within the predicted areas, and interestingly, these sites had yielded

pure PB-1 and Holarctic strains. In contrast, some of the NoAm admixed strains were found in regions that were on the border of suitability in this model (New Brunswick and Wisconsin). In Asia, the model predicts further suitable regions along the Himalayas that are west of known locations.

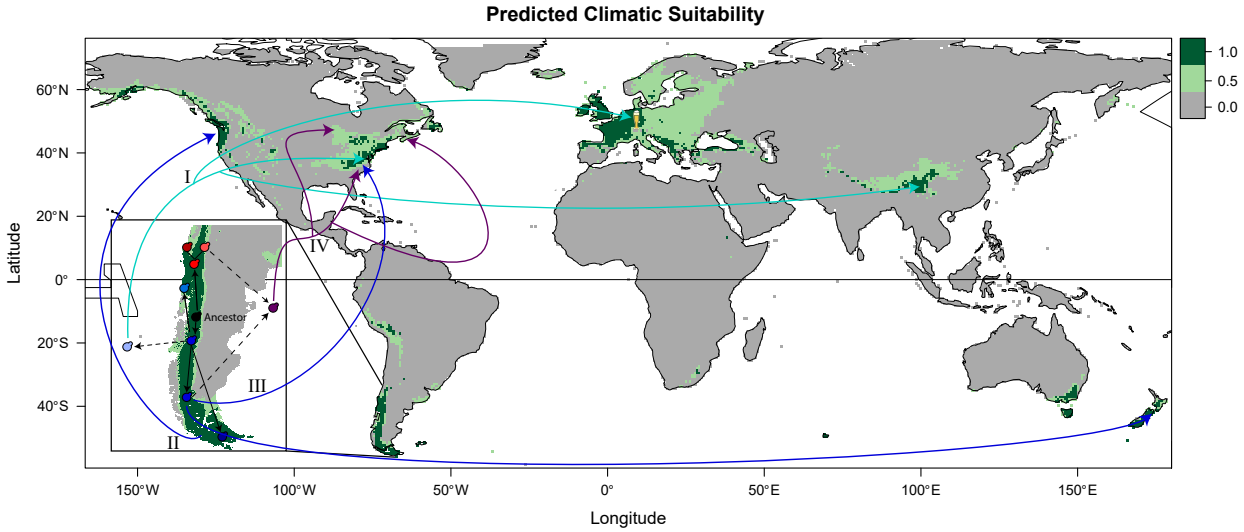

Figure 6. Predicted climatic suitability of *S. eubayanus*.
Minimum training presence (light green) and 10th percentile training presence (dark green) based on a model that includes all known *S. eubayanus* isolations, as well as a scenario of dispersal and diversification out of Patagonia (inset and arrows). Black arrows signify diversification events, dotted lines are diversification events where the population is not found in Patagonia, and colored arrows are migration events for the lineage of matching color. Roman numerals order the potential migration events. *S. eubayanus* has not been found in the wild in Europe, but it has contributed to fermentation hybrids, such as lager yeasts. This scenario proposes that the last common ancestor of PA and PB-Holarctic bifurcated into PA (red) and PB-Holarctic (blue), which further radiated into PA-1 (dark red), PA-2 (light red), PB-1 (blue), PB-2 (lighter blue), PB-3 (dark blue), and Holarctic (very light blue). At least four migration events are needed to explain the locations where *S. eubayanus* has been found. I. The Holarctic subpopulation was drawn from the PB-Holarctic gene pool and colonized the Holarctic ecozone. II. PB-1 colonized the Pacific Rim, including New Zealand and Washington state, USA. III. An independent dispersal event brought PB-1 to North Carolina, USA. IV. Outcrossing between PA-2 and PB-1 gave rise to a low-diversity admixed linage that has recently invaded a large swath of North America.

The uneven global distribution of *S. eubayanus* led us to test if models were robust to being built only with the South American locations or only with the non-South American locations (Figure S9). Remarkably, with just the South American isolates, the model (AIC=1327.32) accurately predicted the locations of the non-South American isolates (Figure

S9A). Even the model built from the limited number of isolates from outside South America (AIC=558.58) still performed reasonably well, identifying the regions in Patagonia along the Andes where *S. eubayanus* has been found (Figure S9B). Collectively, these models suggest that climatic modeling can predict other suitable regions for eukaryotic microbes. These approaches could be used to direct future sampling efforts or applied to other microbes to gain further insight into microbial ecology.

Notably, all models agree that Europe is climatically a prime location for *S. eubayanus* (Figure S9C), but no pure isolates have ever been found there, only hybrids with *S. uvarum*, *S. cerevisiae*, or hybrids with even more parents (Almeida et al. 2014). These hybrids with complex ancestries have been found in numerous fermentation environments, suggesting that pure *S. eubayanus* once existed, or still exists at low abundance or in obscure locations, in Europe. Thus, the lack of wild isolates from sampling efforts in Europe remains a complex puzzle.

Discussion:

Here, we integrated genomic, geographic, and phenotypic data for 200 strains of *S. eubayanus*, the largest collection to date, to gain insight into its world-wide distribution, climatic suitability, and population structure. All the strains belong to the two major populations previously described (Peris et al. 2014, 2016), but with the extended dataset, we were able to define considerable additional structure, consisting of six subpopulations and two admixed lineages. These subpopulations have high genetic diversity, high F_{ST}, and long LD decay; all measures indicative of large and partly isolated populations undergoing limited gene flow. Despite this high genetic diversity, there was relatively little phenotypic differentiation between subpopulations. This dichotomy between large genetic diversity and limited phenotypic

409 differentiation hints at a complex demographic history where genetically differentiated
410 subpopulations are minimally phenotypically differentiated and grow well in a wide range of
411 environments.

412 Despite the strong population structure, we also observed considerable evidence of
413 admixture and gene flow. The two recently admixed lineages had nearly equal contributions
414 from the two major populations, but they were the result of independent outcrossing events. The
415 SoAm admixed strain was isolated from a hotspot of diversity and contains contributions from
416 three subpopulations. The NoAm admixed lineage has spread across at least four distant
417 locations, but all strains descended from the same outcrossing event. Since PA has only been
418 isolated in South America, it is intriguing that the NoAm admixed lineage has been successful in
419 so many locations throughout North America. The success of this lineage could be partially
420 explained by its equal or better performance in many environments in comparison to its parental
421 populations (Fig. 2), perhaps contributing to its invasion of several new locations. Several other
422 Patagonian strains also revealed more modest degrees of gene flow between PA and PB. Finally,
423 we characterized a shared nuclear introgression from *S. uvarum* into four Patagonian strains of *S.*
424 *eubayanus*, demonstrating that hybridization and backcrossing between these sister species has
425 occurred in the wild in South America.

426 *S. eubayanus* has a paradoxical biogeographical distribution; it is abundant in Patagonia,
427 but it is sparsely found elsewhere with far-flung isolates from North America, Asia, and Oceania.
428 Most subpopulations displayed isolation by distance, but genetic diversity only scaled with
429 geographic range to a limited extent. In Patagonia, some sampling sites harbor more genetic
430 diversity than all non-Patagonian locations together (Figure 5B). Although we found the most
431 genetic diversity and largest number of subpopulations north of 43°S, the pattern of genetic

diversity appears to be reversed on the west side of the Andes, at least for the PB-1 subpopulation (Nespolo et al. 2019). This discrepancy could be due to differences in how glacial refugia were distributed (Sérsic et al. 2011) and limitations on gene flow between the east and west sides of the Andes. Together, the levels of *S. eubayanus* genetic diversity found within Patagonia, as well as the restriction of four subpopulations to Patagonia, suggest that Patagonia is the origin of most of the diversity of *S. eubayanus*, likely including the last common ancestor of the PA and PB-Holarctic populations.

The simplest scenario to explain the current distribution and diversity of *S. eubayanus* is a series of radiations in Patagonia, followed by a handful of out-of-Patagonia migration events (Figure 6). Under this model, PA and PB would have bifurcated in Patagonia, possibly in separate glacial refugia. The oldest migration event would have been the dispersal of the ancestor of the Holarctic subpopulation, drawn from the PB gene pool, to the Northern Hemisphere. Multiple more recent migration events could have resulted in the few PB-1 strains found in New Zealand and the USA. The New Zealand and Washington state strains cluster phylogenetically and could have diversified from the same migration event from Patagonia into the Pacific Rim. The PB-1 strain from North Carolina (yHKB35) is genetically more similar to PB-1 strains from Patagonia, suggesting it arrived in the Northern Hemisphere independently of the Pacific Rim strains. Finally, the NoAm admixed strains are likely the descendants of a single, and relatively recent, out-of-Patagonia dispersal. Given that PA appears to be restricted to northern Patagonia, this region could have been where the hybridization leading to the NoAm lineage occurred. While the dispersal vector that brought this admixed lineage to North America is unknown, its far-flung distribution and low diversity show that it has rapidly succeeded by invading new environments.

Other more complex scenarios could conceivably explain the limited number of strains found outside of Patagonia. For example, PA and PB could represent sequential colonizations of Patagonia from the Northern Hemisphere. Under this model, PA would have arrived first and would then have been restricted to northern Patagonia by competition with the later arrival of PB. The Holarctic subpopulation could be interpreted as remnants of the PB population that did not migrate to Patagonia; but the PB-1 strains from the Northern Hemisphere, especially yHKB35, seem far more likely to have been drawn from a Patagonian gene pool than the other way around. Furthermore, the structuring of the PA-1 and the PA-2 subpopulations and of the PB-1, PB-2, and PB-3 subpopulations are particularly challenging to rectify with models that do not allow for diversification within South America. Even more complex scenarios remain possible, and more sampling and isolation will be required to fully elucidate the distribution of this elusive species and more conclusively reject potential biogeographical models.

S. eubayanus has a strikingly parallel population structure and genetic diversity to its sister species *S. uvarum* (Almeida et al. 2014; Peris et al. 2016). Both species are abundant and diverse in Patagonia but can be found globally. Both have early diverging lineages, found in Asia or Australasia, that border on being considered novel species. In South America, both have two major populations, where one of these populations is restricted to northern Patagonia (north of 43°S). However, a major difference between the distribution of these species is that pure strains of *S. uvarum* have been found in Europe. Many dimensions of biodiversity could be interacting to bound the distribution and population structure of both *S. eubayanus* and *S. uvarum*. In particular, we know very little about local ecology, including the biotic community and availability of abiotic resources on a microbial scale, but these factors likely all influence microbial success. We show here that substrate and host association vary between

478 subpopulations. In Patagonia, *S. eubayanus* and *S. uvarum* are commonly associated with
479 *Nothofagus*, where *N. dombeyi* is the preferred host of *S. uvarum* (Libkind et al. 2011; Eizaguirre
480 et al. 2018). Therefore, niche partitioning of host trees could be playing role in the persistence of
481 these species in sympatry in Patagonia. However, in locations where *Nothofagus* is not found and
482 there are perhaps fewer hosts, competitive exclusion between the sister species *S. eubayanus* and
483 *S. uvarum*, could influence distribution. Competition for a narrower set of hosts could potentially
484 explain why only *S. uvarum* has been found in Europe as pure strains, while *S. eubayanus* has
485 not. A second factor influencing distribution and population structure could be dispersal. Yeasts
486 could migrate via many avenues, such as wind, insect, bird, or other animals (Francesca et al.
487 2012, 2014; Stefanini et al. 2012; Gillespie et al. 2012). Human mediated-dispersal has been
488 inferred for the *S. cerevisiae* Wine and Beer lineages and for the *S. paradoxus* European/SpA
489 lineage (Gallone et al. 2016; Gonçalves et al. 2016; Leducq et al. 2014; Kuehne et al. 2007). A
490 third bounding factor could be a region's historical climate. Glacial refugia act as reservoirs of
491 isolated genetic diversity that allow expansion into new areas after glacial retreat (Stewart and
492 Lister 2001). 43°S is a significant geographic boundary due to past geological and climatic
493 variables (Mathiasen and Premoli 2010; Eizaguirre et al. 2018), and many other species and
494 genera show a distinction between their northern and southern counterparts, including
495 *Nothofagus* (Mathiasen and Premoli 2010; Premoli et al. 2012). *S. eubayanus* and *S. uvarum*
496 diversities are also strongly affected by the 43°S boundary (Almeida et al. 2014; Eizaguirre et al.
497 2018), and it seems likely that the microbes experienced some of the same glaciation effects as
498 their hosts. The strong correlation of *S. eubayanus* and *S. uvarum* population structures with
499 43°S further implies a longstanding and intimate association with Patagonia.

The sparse global distribution and complex patterns of genetic diversity continue to raise questions about the niche and potential range of *S. eubayanus*. Our climatic modeling suggests that parts of Europe would be ideal for *S. eubayanus*. Despite extensive sampling efforts, *S. eubayanus* has never been isolated in Europe (Sampaio 2018). However, recent environmental sequencing of the fungal specific ITS1 region hinted that *S. eubayanus* may exist in the wild in Europe (Alsammar et al. 2019). Considerable caution is warranted in interpreting this result because the rDNA locus quickly fixes to one parent's allele in interspecies hybrids, there is only a single ITS1 SNP between *S. uvarum* and *S. eubayanus*, and the dataset contained very few reads that mapped to *S. eubayanus*. Still, the prevalence of hybrids with contributions from the Holarctic lineage of *S. eubayanus* found in Europe (Peris et al. 2016) suggests that the Holarctic lineage exists in Europe, or at least existed historically, allowing it to contribute to many independent hybridization events.

The patterns of radiation and dispersal observed here mirror the dynamics of evolution found in other organisms (Czekanski-Moir and Rundell 2019), including humans (Nielsen et al. 2017). *S. eubayanus* and humans harbor diverse and structured populations in sub-Saharan Africa and Patagonia, respectively. In these endemic regions, both species show signals of ancient and recent admixture between these structured populations. Both species have successfully colonized wide swaths of the globe, with the consequence of repeated bottlenecks in genetic diversity. While anatomically modern humans underwent a single major out-of-Africa migration that led to the peopling of the world (Nielsen et al. 2017), *S. eubayanus* has experienced several migration events from different populations that have led to more punctate global distribution. For both species, intraspecific admixture and interspecific hybridization appear to have played adaptive roles in the success of colonizing these new locations. In humans,

523 introgressions from past hybridizations with both Neanderthals and Denisovans underlie many
524 adaptive traits (Racimo et al. 2015), while the cold fermentation of lager-brewing would not be
525 possible without the cryotolerance of *S. eubayanus* and the aggressive fermentation of
526 domesticated ale strains of *S. cerevisiae* (Gibson and Liti 2015). These parallels illustrate how
527 the biogeographical and evolutionary dynamics observed in plants and animals also shape
528 microbial diversity. As yeast ecology and population genomics (Marsit et al. 2017; Yurkov
529 2017) move beyond the Baas-Becking "Everything is everywhere" hypothesis of microbial
530 ecology (Baas-Becking 1934; de Wit and Bouvier 2006), the rich dynamics of natural diversity
531 that is hidden in the soil at our feet is being uncovered.
532
533 Methods:
534 Wild strain isolations
535 All South American isolates were sampled, isolated, and identified as described
536 previously (Libkind et al. 2011; Eizaguirre et al. 2018). North American isolates new to this
537 publication were from soil or bark samples from the American states of Washington, Wisconsin,
538 North Carolina, and South Carolina (Table S1). Strain enrichment and isolation was done as
539 previously described (Sylvester et al. 2015; Peris et al. 2016, 2014), with a few exceptions in
540 temperature and carbon source of isolation (Table S1). Specifically, two strains were isolated at
541 4°C, eight strains were isolated at room temperature, and six strains were isolated on a non-
542 glucose carbon source: three in galactose, two in sucrose, and one in maltose (Table S1).
543
544 Whole genome sequencing and SNP-calling

Whole genome sequencing was completed with Illumina paired-end reads as described previously (Peris et al. 2016; Shen et al. 2018). Reads were aligned to the reference genome (Baker et al. 2015), SNPs were called, masked for low coverage, and retained for downstream analysis as described previously (Peris et al. 2016). One strain, yHCT75, had more than 20,000 heterozygous SNPs called. This strain was pseudo-phased using read-backed phasing in GATK (McKenna et al. 2010) and split into two phases. Short-read data is deposited in the NCBI Short Read Archive under PRJNA555221.

Population genomic analyses:

Population structure was defined using several approaches: `fastSTRUCTURE` (Raj et al. 2014), `fineSTRUCTURE` (Lawson et al. 2012), `SplitsTree v4` (Huson and Bryant 2006), and Principal Component Analysis with the *adegenet* package in `R` (Jombart 2008). `fineSTRUCTURE` analysis was completed using all strains and 11994 SNPs. The `SplitsTree` network was built with this same set of strains and SNPs. `fastStructure` analysis was completed with as subsample of 5 NoAm strains and 150165 SNPs. We tested K=1 through K=10 and selected K=6 using the "`chooseK.py`" command in `fastSTRUCTURE`. All calculations of pairwise divergence, F_{ST}, and Tajima's D for subpopulations were computed using the `R` package *PopGenome* (Pfeifer and Wittelsbuerger 2015) in windows of 50-kbp. Pairwise divergence between strains was calculated across the whole genome using *PopGenome*. LD was calculated using `PopLDdecay` (Zhang et al. 2019). Geographic area and distance of subpopulations was calculated using the *geosphere* package in `R` (Hijmans et al. 2019). The Mantel tests were completed using *ade4* package of `R` (Dray and Dufour 2007). The F_{ST} network was built with *iGraph* in `R` (Csardi and Nepusz 2006).

568

569 Niche projection with Wallace:

570 Climatic modeling of *S. eubayanus* was completed using the `R` package *Wallace* (Kass et
571 al. 2018). Three sets of occurrence data were tested: one that included only GPS coordinates for
572 strains from South America, one that included only non-South American isolates, and one that
573 included all known isolates (Table S1). We could use exact GPS coordinates for most strains,
574 except for the strains from East Asia, where we estimated the locations (Bing et al. 2014).
575 WorldClim bioclimatic variables were obtained at a resolution of 2.5 arcmin. The background
576 extent was set to "Minimum convex polygon" with a 0.5-degree buffer distance and 10,000
577 background points were sampled. We used block spatial partitioning. The model was built using
578 the Maxent algorithm, using the feature classes: L (linear), LQ (linear quadradic), H (Hinge),
579 LQH, and LQHP (Linear Quadradic Hinge Product) with 1-3 regularization multipliers and the
580 multiplier step value set to 1. The model was chosen based on the Akaike Information Criterion
581 (AIC) score (Table S5). The best models were then projected to the all continents, except
582 Antarctica.

583

584 Phenotyping:

585 Strains were first revived in Yeast Peptone Dextrose (YPD) and grown for 3 days at room
586 temperature. These saturated cultures were then transferred to two 96-well microtiter plates, for
587 growth rate and stress tolerance phenotyping. These plates were incubated overnight. Cells were
588 pinned from these plates into plates for growth rate measurements. For temperature growth
589 assays, cells were pinned into four fresh YPD microtiter plates and then incubated at 0°C, 4°C,
590 10°C, and 20°C. For the microtiter plates at 0°C, 4°C, and 10°C, OD was measured at least once

a day for two weeks or until a majority of the strains had reached stationary phase. Growth on different carbon sources was measured at 20°C in MM media with 2% of the respective carbon source. Carbon sources tested were: glucose, galactose, raffinose, maltose, maltotriose, ethanol, and glycerol. OD was read every two hours for one week or until saturation. All phenotyping was completed in biological triplicate. The carbon source data was truncated to 125 hours to remove artifacts due to evaporation. Growth curves were analyzed using the package *grofit* (Kahm et al. 2010) in `R` to measure saturation and growth rate. We then averaged each strain over the triplicates. We used an ANOVA corrected with Tukey's HSD to test for growth rate interactions between subpopulation and carbon source or subpopulation and temperature. We used the `R` package *pvclust* (Suzuki and Shimodaira 2006) to cluster and build heatmaps of growth rate by subpopulation.

Heat shock was completed by pelleting 200µl saturated culture, removing supernatant, resuspending in 200µl YPD pre-heated to 37°C, and incubating for one hour at 37°C, with a room temperature control. Freeze-thaw tolerance was tested by placing saturated YPD cultures in a dry ice ethanol bath for two hours, with a control that was incubated on ice. After stress, the strains were serially diluted 1:10 three times and pinned onto solid YPD. These dilution plates were then photographed after 6 and 18 hours. `CellProfiler` (Lamprecht et al. 2007) was used to calculate the colony sizes after 18 hours, and the 3rd (1:1000) dilutions were used for downstream analyses. The heat shock measurements were normalized by the room temperature controls, and the freeze thaw measurements were normalized by the ice incubation controls. Statistical interactions of subpopulations and stress responses were tested as above.

Data Availability:

614 All short-read genome sequencing data has been deposited in the NCBI Short Read Archive
615 under the PRJNA555221. Accessions of public data is given in Table S1.
616
617 Acknowledgements:
618 We thank Francisco A. Cubillos for coordinating publication with their study; Sean D. Schoville,
619 José Paulo Sampaio, Paula Gonçalves, and members of the Hittinger Lab, in particular
620 EmilyClare P. Baker, for helpful discussion and feedback; Amanda B. Hulfachor and Martin
621 Bontrager for preparing a subset of Illumina libraries; the University of Wisconsin
622 Biotechnology Center DNA Sequencing Facility for providing Illumina sequencing facilities and
623 services; the Agricultural Research Service (ARS) NRRL collection, Christian R. Landry,
624 Ashley Kinart, and Drew T. Doering for strains included in phenotyping; Huu-Vang Nguyen for
625 strains used for hybrid genome comparison; and Leslie Shown, Anita R. & S. Todd Hittinger,
626 EmilyClare P. Baker, and Ryan V. Moriarty for collecting samples and/or isolating strains. This
627 material is based upon work supported by the National Science Foundation under Grant Nos.
628 DEB-1253634 (to CTH) and DGE-1256259 (Graduate Research Fellowship to QKL), the USDA
629 National Institute of Food and Agriculture Hatch Project No. 1003258 to CTH, and in part by the
630 DOE Great Lakes Bioenergy Research Center (DOE BER Office of Science Nos. DE-
631 SC0018409 and DE-FC02-07ER64494 to Timothy J. Donohue). QKL was also supported by the
632 Predoctoral Training Program in Genetics, funded by the National Institutes of Health
633 (5T32GM007133). DP is a Marie Sklodowska-Curie fellow of the European Union's Horizon
634 2020 research and innovation program (Grant Agreement No. 747775). DL was supported by
635 CONICET (PIP11220130100392CO), FONCyT (PICT 3677, PICT 2542), Universidad Nacional
636 del Comahue (B199), and NSF-CONICET grant. CTH is a Pew Scholar in the Biomedical

637 Sciences and H. I. Romnes Faculty Fellow, supported by the Pew Charitable Trusts and Office of
638 the Vice Chancellor for Research and Graduate Education with funding from the Wisconsin
639 Alumni Research Foundation (WARF), respectively.

640

641 Author Contributions:

642 QKL, DL, and CTH, conceived of the study; QLK, DP, JIE, DL, and CTH refined concept and
643 design; QKL performed all population genomic and ecological niche analyses; QKL and DAO
644 sequenced genomes, performed phenotyping and statistical analyses, and mentored KVB and
645 MJ; DL and CTH supervised the study; KVB, KS, and MJ isolated and/or identified North
646 American strains; JIE, MER, CAL, and DL isolated and/or provided South American strains; and
647 QKL and CTH wrote the manuscript with editorial input from all co-authors.

648

649 Conflict of Interest Disclosure:

650 Commercial use of *Saccharomyces eubayanus* strains requires a license from WARF or
651 CONICET. Strains are available for academic research under a material transfer agreement.

652

653 References:

654 Almeida P, Gonçalves C, Teixeira S, Libkind D, Bontrager M, Masneuf-Pomarède I, Albertin W,
655 Durrens P, Sherman DJ, Marullo P, et al. 2014. A Gondwanan imprint on global diversity
656 and domestication of wine and cider yeast *Saccharomyces uvarum*. *Nat Commun* **5**: 4044.
657 Alsammar HF, Naseeb S, Brancia LB, Gilman RT, Wang P, Delneri D. 2019. Targeted
658 metagenomics approach to capture the biodiversity of *Saccharomyces* genus in wild
659 environments. *Environ Microbiol Rep* **11**: 206–214.
660 Baas-Becking L. 1934. *Geobiologie; of inleiding tot de milieukunde*. WP Van Stockum & Zoon
661 NV.
662 Baker E, Wang B, Bellora N, Peris D, Hulfachor AB, Koshalek JA, Adams M, Libkind D,
663 Hittinger CT. 2015. The genome sequence of Saccharomyces eubayanus and the
664 domestication of lager-brewing yeasts. *Mol Biol Evol* **32**: 2818–2831.
665 Baker EP, Peris D, Moriarty R V, Li XC, Fay JC, Hittinger CT. 2019. Mitochondrial DNA and
666 temperature tolerance in lager yeasts. *Sci Adv* **5**: eaav1869.

667 Bing J, Han P-J, Liu W-Q, Wang Q-M, Bai F-Y. 2014. Evidence for a Far East Asian origin of
668 lager beer yeast. *Curr Biol* **24**: R380-1.
669 Brouwers N, Brickwedde A, Gorter de Vries AR, van den Broek M, Weening SM, van den
670 Eijnden L, Diderich JA, Bai F-Y, Pronk JT, Daran J-MG. 2019. Maltotriose consumption
671 by hybrid *Saccharomyces pastorianus* is heterotic and results from regulatory cross-talk
672 between parental sub-genomes. *bioRxiv* 679563.
673 Csardi G, Nepusz T. 2006. The igraph software package for complex network research.
674 *InterJournal* **1695**: 1–9.
675 Czekanski-Moir JE, Rundell RJ. 2019. The Ecology of Nonecological Speciation and
676 Nonadaptive Radiations. *Trends Ecol Evol* **34**: 400–415.
677 de Wit R, Bouvier T. 2006. "Everything is everywhere, but, the environment selects"; what did
678 Baas Becking and Beijerinck really say? *Environ Microbiol* **8**: 755–758.
679 Dray S, Dufour A-B. 2007. The ade4 Package: Implementing the Duality Diagram for
680 Ecologists. *J Stat Softw* **22**: 1–20.
681 Eberlein C, Hénault M, Fijarczyk A, Charron G, Bouvier M, Kohn LM, Anderson JB, Landry
682 CR. 2019. Hybridization is a recurrent evolutionary stimulus in wild yeast speciation. *Nat*
683 *Commun* **10**.
684 Eizaguirre JI, Peris D, Rodríguez ME, Lopes CA, De Los Ríos P, Hittinger CT, Libkind D. 2018.
685 Phylogeography of the wild Lager-brewing ancestor (*Saccharomyces eubayanus*) in
686 Patagonia. *Environ Microbiol* **20**: 3732–3743.
687 Francesca N, Canale DE, Settanni L, Moschetti G. 2012. Dissemination of wine-related yeasts by
688 migratory birds. *Environ Microbiol Rep* **4**: 105–112.
689 Francesca N, Carvalho C, Sannino C, Guerreiro M a, Almeida PM, Settanni L, Massa B,
690 Sampaio JP, Moschetti G. 2014. Yeasts vectored by migratory birds collected in the
691 Mediterranean island of Ustica and description of *Phaffomyces usticensis* f.a. sp. nov., a
692 new species related to the cactus ecoclade. *FEMS Yeast Res* **14**: 910–21.
693 Gallone B, Steensels J, Prahl T, Soriaga L, Saels V, Herrera-Malaver B, Merlevede A,
694 Roncoroni M, Voordeckers K, Miraglia L, et al. 2016. Domestication and Divergence of
695 *Saccharomyces cerevisiae* Beer Yeasts. *Cell* **166**: 1397-1410.e16.
696 Gayevskiy V, Goddard MR. 2016. *Saccharomyces eubayanus* and *Saccharomyces arboricola*
697 reside in North Island native New Zealand forests. *Environ Microbiol* **18**: 1137–1147.
698 Gibson B, Liti G. 2015. *Saccharomyces pastorianus*: genomic insights inspiring innovation for
699 industry. *Yeast* **32**: 17–27.
700 Gibson BR, Storgårds E, Krogerus K, Vidgren V. 2013. Comparative physiology and
701 fermentation performance of Saaz and Frohberg lager yeast strains and the parental species
702 *Saccharomyces eubayanus*. *Yeast* **30**: 255–266.
703 Gillespie RG, Baldwin BG, Waters JM, Fraser CI, Nikula R, Roderick GK. 2012. Long-distance
704 dispersal: a framework for hypothesis testing. *Trends Ecol Evol* **27**: 47–56.
705 Gonçalves M, Pontes A, Almeida P, Barbosa R, Serra M, Libkind D, Hutzler M, Gonçalves P,
706 Sampaio JP. 2016. Distinct Domestication Trajectories in Top- Fermenting Beer Yeasts and
707 Wine Yeasts. *Curr Biol* **26**: 1–12.
708 Hijmans RJ, Williams E, Vennes C. 2019. *Package "geosphere" Type Package Title Spherical*
709 *Trigonometry*.
710 Hittinger CT. 2013. *Saccharomyces* diversity and evolution: a budding model genus. *Trends*
711 *Genet* **29**: 309–17.
712 Hittinger CT, Steele JL, Ryder DS. 2018. Diverse yeasts for diverse fermented beverages and

foods. *Curr Opin Biotechnol* **49**: 199–206.
Huson DH, Bryant D. 2006. Application of Phylogenetic Networks in Evolutionary Studies. *Mol Biol Evol* **23**: 254–267.
Jombart T. 2008. adegenet: a R package for the multivariate analysis of genetic markers. *Bioinformatics* **24**: 1403–1405.
Kahm M, Hasenbrink G, Lichtenberg-Fraté H, Ludwig J, Kschischo M. 2010. grofit : Fitting Biological Growth Curves with R. *J Stat Softw* **33**: 1–21.
Kass JM, Vilela B, Aiello-Lammens ME, Muscarella R, Merow C, Anderson RP. 2018. Wallace : A flexible platform for reproducible modeling of species niches and distributions built for community expansion ed. R.B. O'Hara. *Methods Ecol Evol* **9**: 1151–1156.
Kuehne HA, Murphy HA, Francis CA, Sniegowski PD. 2007. Allopatric Divergence, Secondary Contact, and Genetic Isolation in Wild Yeast Populations. *Curr Biol* **17**: 407–411.
Lamprecht MR, Sabatini DM, Carpenter AE. 2007. CellProfiler™: Free, versatile software for automated biological image analysis. *Biotechniques* **42**: 71–75.
Lawson DJ, Hellenthal G, Myers S, Falush D. 2012. Inference of population structure using dense haplotype data. *PLoS Genet* **8**: e1002453.
Leducq J-B, Charron G, Samani P, Dubé AK, Sylvester K, James B, Almeida P, Sampaio JP, Hittinger CT, Bell G, et al. 2014. Local climatic adaptation in a widespread microorganism. *Proc Biol Sci* **281**: 20132472.
Leducq J-B, Nielly-Thibault L, Charron G, Eberlein C, Verta J-P, Samani P, Sylvester K, Hittinger CT, Bell G, Landry CR. 2016. Speciation driven by hybridization and chromosomal plasticity in a wild yeast. *Nat Microbiol* **1**: 1–10.
Libkind D, Hittinger CT, Valério E, Gonçalves C, Dover J, Johnston M, Gonçalves P, Sampaio JP. 2011. Microbe domestication and the identification of the wild genetic stock of lager-brewing yeast. *Proc Natl Acad Sci U S A* **108**: 14539–44.
Liti G, Carter DM, Moses AM, Warringer J, Parts L, James SA, Davey RP, Roberts IN, Burt A, Koufopanou V, et al. 2009. Population genomics of domestic and wild yeasts. *Nature* **458**: 337–341.
Marsit S, Leducq JB, Durand É, Marchant A, Filteau M, Landry CR. 2017. Evolutionary biology through the lens of budding yeast comparative genomics. *Nat Rev Genet* **18**: 581–598.
Mathiasen P, Premoli AC. 2010. Out in the cold: Genetic variation of *Nothofagus pumilio* (Nothofagaceae) provides evidence for latitudinally distinct evolutionary histories in austral South America. *Mol Ecol* **19**: 371–385.
McKenna A, Hanna M, Banks E, Sivachenko A, Cibulskis K, Kernytsky A, Garimella K, Altshuler D, Gabriel S, Daly M, et al. 2010. The Genome Analysis Toolkit: A MapReduce framework for analyzing next-generation DNA sequencing data. *Genome Res* **20**: 1297–1303.
Naseeb S, Alsammar H, Burgis T, Donaldson I, Knyazev N, Knight C, Delneri D. 2018. Whole Genome Sequencing, de Novo Assembly and Phenotypic Profiling for the New Budding Yeast Species *Saccharomyces jurei*. *G3* **8**: 2967–2977.
Nespolo RF, Villarroel CA, Oporto CI, Tapia SM, Vega F, Urbina K, De Chiara M, Mozzachiodi S, Mikhalev E, Thompson D, et al. 2019. An Out-of-Patagonia dispersal explains most of the worldwide genetic distribution in *Saccharomyces eubayanus*. *Submiss*.
Nguyen HV, Boekhout T. 2017. Characterization of *Saccharomyces uvarum* (Beijerinck, 1898) and related hybrids: Assessment of molecular markers that predict the parent and hybrid genomes and a proposal to name yeast hybrids. *FEMS Yeast Res* **17**: 1–19.

759 Nielsen R, Akey JM, Jakobsson M, Pritchard JK, Tishkoff S, Willerslev E. 2017. Tracing the
760 peopling of the world through genomics. *Nature* **541**: 302–310.
761 Peris D, Langdon QK, Moriarty R V, Sylvester K, Bontrager M, Charron G, Leducq JB, Landry
762 CR, Libkind D, Hittinger CT. 2016. Complex Ancestries of Lager-Brewing Hybrids Were
763 Shaped by Standing Variation in the Wild Yeast *Saccharomyces eubayanus*. *PLoS Genet*
764 **12**.
765 Peris D, Sylvester K, Libkind D, Gonçalves P, Sampaio JP, Alexander WG, Hittinger CT. 2014.
766 Population structure and reticulate evolution of *Saccharomyces eubayanus* and its lager-
767 brewing hybrids. *Mol Ecol* **23**: 2031–2045.
768 Peter J, De Chiara M, Friedrich A, Yue JX, Pflieger D, Bergström A, Sigwalt A, Barre B, Freel
769 K, Llored A, et al. 2018. Genome evolution across 1,011 *Saccharomyces cerevisiae* isolates.
770 *Nature* **556**: 339–344.
771 Pfeifer B, Wittelsbuerger U. 2015. Package 'PopGenome .'
772 Premoli AC, Mathiasen P, Cristina Acosta M, Ramos VA. 2012. Phylogeographically
773 concordant chloroplast DNA divergence in sympatric *Nothofagus s.s.* How deep can it be?
774 *New Phytol* **193**: 261–275.
775 Premoli AC, Mathiasen P, Kitzberger T. 2010. Southern-most *Nothofagus* trees enduring ice
776 ages: Genetic evidence and ecological niche retrodiction reveal high latitude (54°S) glacial
777 refugia. *Palaeogeogr Palaeoclimatol Palaeoecol* **298**: 247–256.
778 Quiroga MP, Premoli AC. 2010. Genetic structure of *Podocarpus nubigena* (Podocarpaceae)
779 provides evidence of Quaternary and ancient historical events. *Palaeogeogr Palaeoclimatol*
780 *Palaeoecol* **285**: 186–193.
781 Racimo F, Sankararaman S, Nielsen R, Huerta-Sánchez E. 2015. Evidence for archaic adaptive
782 introgression in humans. *Nat Rev Genet* **16**: 359–371.
783 Raj A, Stephens M, Pritchard JK. 2014. fastSTRUCTURE: Variational Inference of Population
784 Structure in Large SNP Data Sets. *Genetics* **197**: 573–589.
785 Rodríguez ME, Pérez-Través L, Sangorrín MP, Barrio E, Lopes CA. 2014. *Saccharomyces*
786 *eubayanus* and *Saccharomyces uvarum* associated with the fermentation of *Araucaria*
787 *araucana* seeds in Patagonia. *FEMS Yeast Res* **14**: 948–965.
788 Salema-Oom M, Pinto VV, Gonçalves P, Spencer-Martins I. 2005. Maltotriose Utilization by
789 Industrial. *Society* **71**: 5044–5049.
790 Sampaio JP. 2018. Microbe profile: Saccharomyces eubayanus, the missing link to lager beer
791 yeasts. *Microbiol (United Kingdom)* **164**: 1069–1071.
792 Sampaio JP, Gonçalves P. 2017. Biogeography and Ecology of the Genus *Saccharomyces*. In
793 *Yeasts in Natural Ecosystems: Ecology*, pp. 131–157.
794 Schacherer J, Shapiro JA, Ruderfer DM, Kruglyak L. 2009. Comprehensive polymorphism
795 survey elucidates population structure of *Saccharomyces cerevisiae*. *Nature* **458**: 342–5.
796 Sérsic AN, Cosacov A, Cocucci AA, Johnson LA, Pozner R, Avila LJ, Sites Jr. JW, Morando M.
797 2011. Emerging phylogeographical patterns of plants and terrestrial vertebrates from
798 Patagonia. *Biol J Linn Soc* **103**: 475–494.
799 Shen X-X, Opulente DA, Kominek J, Zhou X, Steenwyk JL, Buh K V., Haase MAB, Wisecaver
800 JH, Wang M, Doering DT, et al. 2018. Tempo and Mode of Genome Evolution in the
801 Budding Yeast Subphylum. *Cell* **175**: 1533-1545.e20.
802 Stefanini I, Dapporto L, Legras J-L, Calabretta A, Di Paola M, De Filippo C, Viola R, Capretti P,
803 Polsinelli M, Turillazzi S, et al. 2012. Role of social wasps in Saccharomyces cerevisiae
804 ecology and evolution. *Proc Natl Acad Sci U S A* **109**: 13398–403.

Stewart JR, Lister AM. 2001. Cryptic northern refugia and the origins of the modern biota. *Trends Ecol Evol* **16**: 608–613.

Suzuki R, Shimodaira H. 2006. Pvclust: An R package for assessing the uncertainty in hierarchical clustering. *Bioinformatics* **22**: 1540–1542.

Sylvester K, Wang Q-M, James B, Mendez R, Hulfachor AB, Hittinger CT. 2015. Temperature and host preferences drive the diversification of *Saccharomyces* and other yeasts: a survey and the discovery of eight new yeast species. *FEMS Yeast Res* **15**: fov002.

Yurkov A. 2017. Temporal and Geographic Patterns in Yeast Distribution. In *Yeasts in Natural Ecosystems: Ecology*, pp. 101–130.

Zhang C, Dong S-S, Xu J-Y, He W-M, Yang T-L. 2019. PopLDdecay: a fast and effective tool for linkage disequilibrium decay analysis based on variant call format files. *Bioinformatics* **35**: 1786–1788.

Figure Legends:

Figure 1. *S. eubayanus* distribution and population structure.

S. eubayanus has a global distribution and two major populations with six subpopulations. (A) Isolation locations of *S. eubayanus* strains included in the dataset. For visibility, circle size is not scaled by the number of strains. Subpopulation abundance is shown as pie charts. The Patagonian sampling sites have been collapsed to two locations for clarity. Details of sites and subpopulations found in South America (B) and North America (C) with circle size scaled by the number of strains. (D) Whole genome PCA of *S. eubayanus* strains and five hybrids with large contributions from *S. eubayanus*. (E) PCA of just PA. (F) PCA of just PB and hybrid *S. eubayanus* sub-genomes. Color legends in A and D apply to this and all other figures.

Figure 2. Phenotypic differences.

(A) Heat map of mean of maximum growth rate (change in OD/hour) (GR) on different carbon sources by subpopulation. Warmer colors designate faster growth. (B) Heat map of $\log_{10}$ normalized growth at different temperatures by subpopulation.

Figure 3. Population genomic parameters.

(A) Network built with pairwise F_{ST} values < 0.8 between each subpopulation. F_{ST} values are printed and correspond to line thickness, where lower values are thicker. Circle sizes correspond to genetic diversity. (B) LD decay for each subpopulation (colors) and the species in whole (black).

Figure 4. Genomic ancestries of NoAm and SoAm admixed lineages.
(A) For all 21 NoAm admixed strains, $\log_2$ ratio of the minimum PB-NoAm pairwise nucleotide sequence divergence (dB-NoAm) and the minimum PA-NoAm pairwise nucleotide sequence divergence (dA-NoAm) in 50-kbp windows. Colors and $\log_2 < 0$ or > 0 indicate that part of the genome is more closely related to PA or PB, respectively. (B) Neighbor-Net phylogenetic network reconstructed with the 571 SNPs that differentiate the NoAm strains. The scale bar represents the number of substitutions per site. Collection location is noted. (C) Pairwise nucleotide sequence divergence of the NoAm strain yHKS210 compared to strains from the PA-1 and PA-2 subpopulations of PA in 50-kbp windows. (D) Pairwise nucleotide sequence divergence of the NoAm strain yHKS210 compared to strains from the PB-1, PB-2, and PB-3 subpopulations of PB in 50-kbp windows. (E) $\log_2$ ratio of the minimum PB-SoAm pairwise nucleotide sequence divergence (dB-SoAm) and the minimum PA-SoAm pairwise nucleotide sequence divergence (dA-SoAm) in 50-kbp windows. Colors and $\log_2 < 0$ or > 0 indicate that part of the genome is more closely related to PA or PB, respectively. (F) Pairwise nucleotide sequence divergence of the SoAm strain compared to strains from the PA-1 and PA-2 subpopulations of PA in 50-kbp windows. (G) Pairwise nucleotide sequence divergence of the SoAm strain compared to strains of the PB-1, PB-2, and PB-3 subpopulations of PB in 50-kbp windows.

Figure 5. South American genomic diversity versus range, diversity by area, and isolation by distance.
(A) Range and genomic diversity of South American sampling sites. Circle sizes correspond to nucleotide diversity of all strains from that site, and pie proportions correspond to each subpopulation's contribution to π at each site. Latitudinal range of each subpopulation is shown to the right. (B) Nucleotide diversity by subpopulation by sampling site, where larger and darker circles indicate more diversity. "SA Sites" in gray show the diversity of all strains found in each South American (SA) site. "World Sites" in darker gray show the nucleotide diversity of all North American or non-South American strains, regardless of subpopulation, compared to South American strains south or north of 43°S, aligned to mean latitude of all strains included in the analysis. (C) Correlation of nucleotide diversity and the area or distance a subpopulation covers. The y-axis shows the nucleotide diversity of each subpopulation, and circle sizes correspond to

871 the geographic sizes of the subpopulations on a log10 scale. Note that PA-1 (dark red) is as
872 diverse as PB-3 (dark blue) but encompasses a smaller area. (D) $\log_{10}$(pairwise nucleotide
873 diversity) correlated with distance between strains, which demonstrates isolation by distance.
874 Note that y-axes are all scaled the same but not the x-axes. Holarctic includes the *S. eubayanus*
875 sub-genome of two lager-brewing strains. Figure S8A shows the individual plots for the NoAm
876 lineage. Figure S8B shows the individual plot of PB-1.
877
878 Figure 6. Predicted climatic suitability of *S. eubayanus*.
879 Minimum training presence (light green) and 10th percentile training presence (dark green) based
880 on a model that includes all known *S. eubayanus* isolations, as well as a scenario of dispersal and
881 diversification out of Patagonia (inset and arrows). Black arrows signify diversification events,
882 dotted lines are diversification events where the population is not found in Patagonia, and
883 colored arrows are migration events for the lineage of matching color. Roman numerals order the
884 potential migration events. *S. eubayanus* has not been found in the wild in Europe, but it has
885 contributed to fermentation hybrids, such as lager yeasts. This scenario proposes that the last
886 common ancestor of PA and PB-Holarctic bifurcated into PA (red) and PB-Holarctic (blue),
887 which further radiated into PA-1 (dark red), PA-2 (light red), PB-1 (blue), PB-2 (lighter blue),
888 PB-3 (dark blue), and Holarctic (very light blue). At least four migration events are needed to
889 explain the locations where *S. eubayanus* has been found. I. The Holarctic subpopulation was
890 drawn from the PB-Holarctic gene pool and colonized the Holarctic ecozone. II. PB-1 colonized
891 the Pacific Rim, including New Zealand and Washington state, USA. III. An independent
892 dispersal event brought PB-1 to North Carolina, USA. IV. Outcrossing between PA-2 and PB-1
893 gave rise to a low-diversity admixed linage that has recently invaded a large swath of North
894 America.
895
896 Supplementary Figure 1. Additional visualizations of population structure.
897 (A) SplitsTree network tree built with 11994 SNPs with subpopulations circled and labeled. (B)
898 FineStructure co-ancestry plot built with 11994 SNPs. Bluer colors correspond to more genetic
899 similarity. Boxes have been added to label the subpopulations. (C) FastSTRUCTURE plot (K=6)
900 built with 150165 SNPs and showing the same six monophyletic subpopulations found with
901 other approaches. Only five NoAm strains were included in the fastSTRUCTURE analysis.

902

903 Supplementary Figure. 2. Additional phenotypic data.

904 (A) Violin plots of recovery from stress, normalized by controls. There were no significant
905 subpopulation by stress interactions. (B) Violin plots of $\log_{10}$ normalized mean growth rates of
906 each subpopulation at 0°C, 4°C, 10°C, and 20°C. * = p-val < 0.05 of interactions between Lager
907 and PA-2, PB-2, and PB-3 at 10°C; Lager and PA-1, PA-2, PB-1, PB-2, and PB-3 at 20°C; and
908 PB-2 and both PA-2 and NoAm at 20°C (C) Violin plots of mean growth rate on different carbon
909 sources (* = p-val < 0.05). (D) Heatmaps of significant subpopulation by temperature
910 interactions and (E) significant subpopulation by carbon source interactions. Warmer colors
911 indicate that the subpopulation-temperature or carbon source on the left hand had a faster growth
912 rate than the subpopulation-temperature or carbon source along the bottom; cooler colors
913 represent the reverse. Non-significant interactions, based on multiple test corrections, are in
914 white. More intense colors represent smaller p-values.

915

916 Supplementary Figure 3. Heterozygosity analyses.

917 (A) Summary of all SNPs vs SNPs called as heterozygous compared to the taxonomic type strain
918 for all 200 strains included in this study. The upper limit of the bar is the total SNP count. The
919 lower point corresponds to SNPs called as heterozygous. The horizontal line is 20k SNPs. (B)
920 Strain yHCT75 (CRUB 1946) is the only strain with > 20K heterozygous SNPs. (C) When the
921 heterozygous SNPs of yHCT75 were pseudo-phased (labeled), both phases clustered with PB-1.

922

923 Supplementary Figure 4. Additional population genomic statistics.

924 (A) Mean pairwise nucleotide diversity (π * 100) for each subpopulation across the genome in
925 50-kbp windows. (B) Tajima's D across the genome in 50-kbp windows for each subpopulation.
926 (C) Mean F_{ST} in 50-kpb windows for each subpopulation compared to all subpopulations. (D)
927 Pairwise F_{ST} for each subpopulation compared to PB-1.

928

929 Supplementary Figure 5. Pairwise F_{ST} plots for NoAm and SoAm compared to all other
930 subpopulations.

931 Pairwise F_{ST} for the NoAm lineage (A) or SoAm strain (B) compared to all other subpopulations.

932

933 Supplementary Figure 6. The taxonomic type strain has a mosaic genome.
934 (A) Pairwise genetic divergence of the taxonomic type strain compared to each subpopulation.
935 (B) Comparison of pairwise genetic divergence of the taxonomic type strain compared to PA-1
936 and PB-1. (C) $\log_2$ divergence plot (as in Figure 4) showing regions introgressed from PA-1 in
937 the taxonomic type strain.
938
939 Supplementary Figure 7. Four *S. eubayanus* strains with *S. uvarum* nuclear introgressions.
940 (A) Depth of coverage plots of reads from four strains mapped to both the *S. uvarum* (Suva) and
941 *S. eubayanus* (Seub) reference genomes. (B) Zoom-in of region on Chromosome XIV where
942 these four strains have the same *S. uvarum* (purple) introgression into a *S. eubayanus*
943 background. (C) A PCA plot shows that these four strains belong to the PB-1 subpopulation of *S.*
944 *eubayanus*. (D) A PCA plot shows that the introgressed region from *S. uvarum* came from the
945 South American SA-B subpopulation of *S. uvarum*.
946
947 Supplementary Figure 8. Isolation by distance plots for NoAm and PB-1.
948 (A) Isolation by distance for all NoAm strains. The y-axis has been rescaled compared to Figure
949 5 for better visualization. (B) Isolation by distance for subpopulation PB-1. Comparisons with
950 strains from Cerro Ñielol are labeled. All comparisons of South American strains with non-South
951 American strains are on the right side.
952
953 Supplementary Figure 9. Additional Wallace climatic models.
954 (A) Model built using only South American isolation locations. (B) Model built using only non-
955 South American sites. (C) Comparison of models based on all known *S. eubayanus* collection
956 sites, only South American, or only non-South American sites. Where the models agree is in dark
957 green, where two models agree is in medium green, and where one model predicts suitability is
958 in light green.
959
960 Supplementary Table 1. Collection information for all strains whose genomes were sequenced or
961 analyzed in this study.
962

963 Supplementary Table 2. Average triplicate growth rates for various temperatures and carbon
964 sources. Note that this spreadsheet has multiple sheets.
965
966 Supplementary Table 3. K=6 output of FastSTRUCTURE.
967
968 Supplementary Table 4. Mantel test results.
969
970 Supplementary Table 5. Input and output for Wallace climatic modeling.

Figure 1

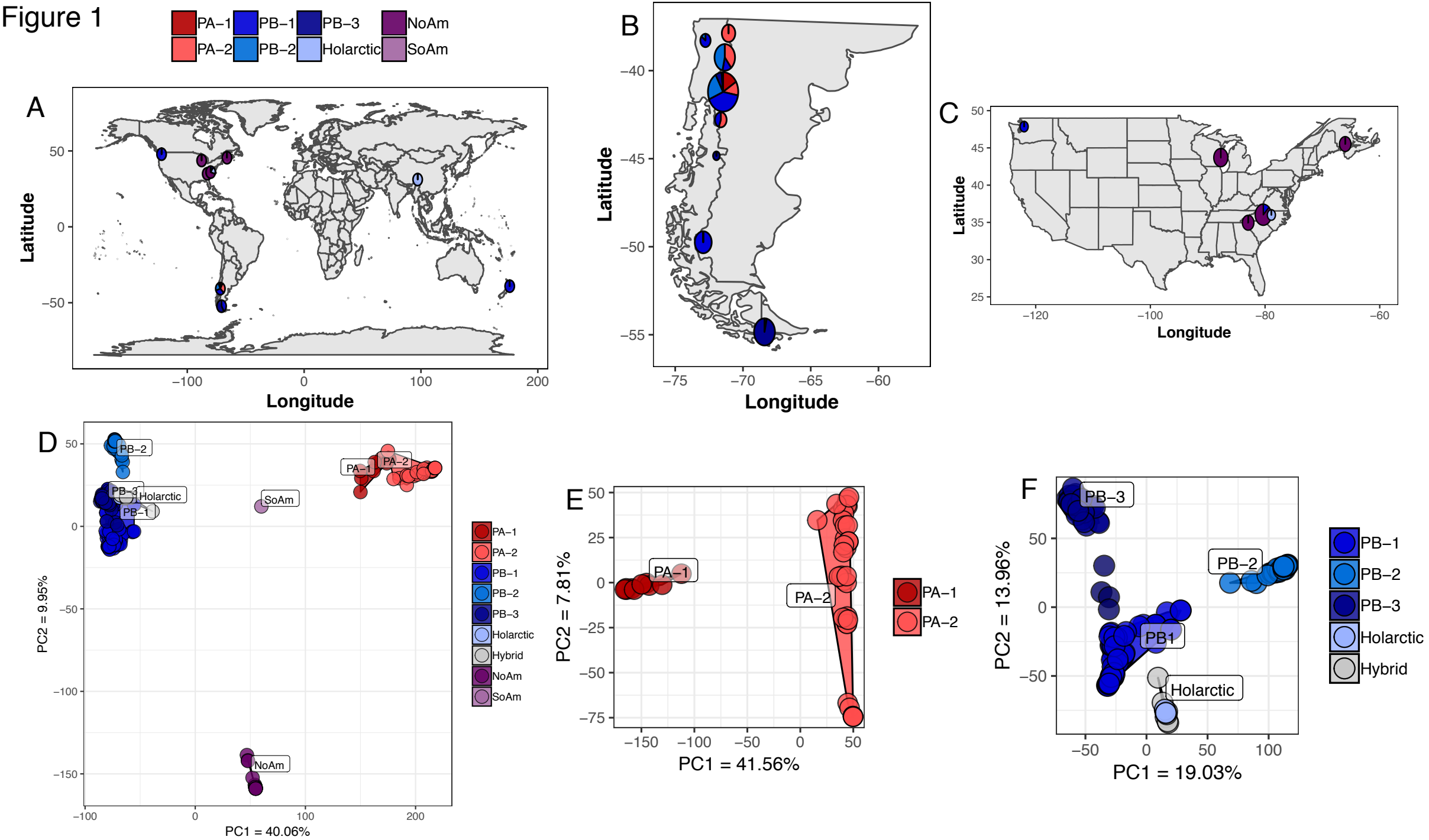
PA–1
PA–2
PB–1
PB–2
PB–3
Holarctic
NoAm
SoAm
A
Latitude
Longitude
B
C
D
PC2 = 9.95%
PC1 = 40.06%
Hybrid
E
PC2 = 7.81%
PC1 = 41.56%
F
PC2 = 13.96%
PC1 = 19.03%
PB1

Figure 2

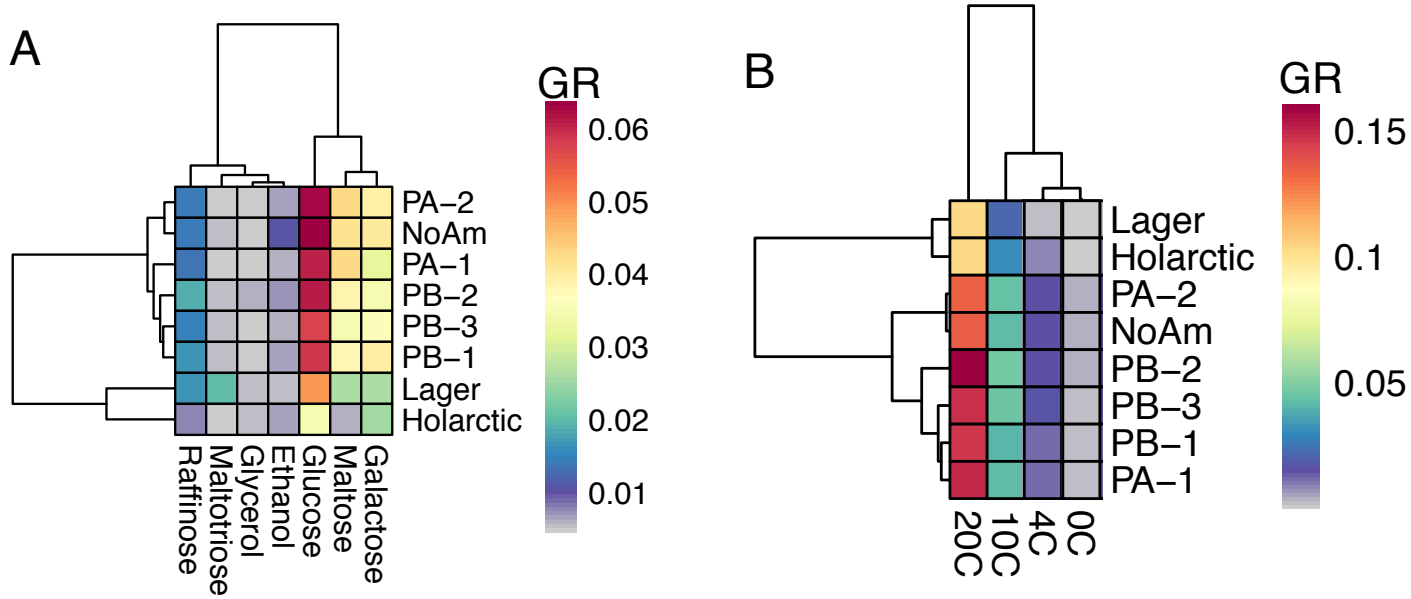

Figure 3

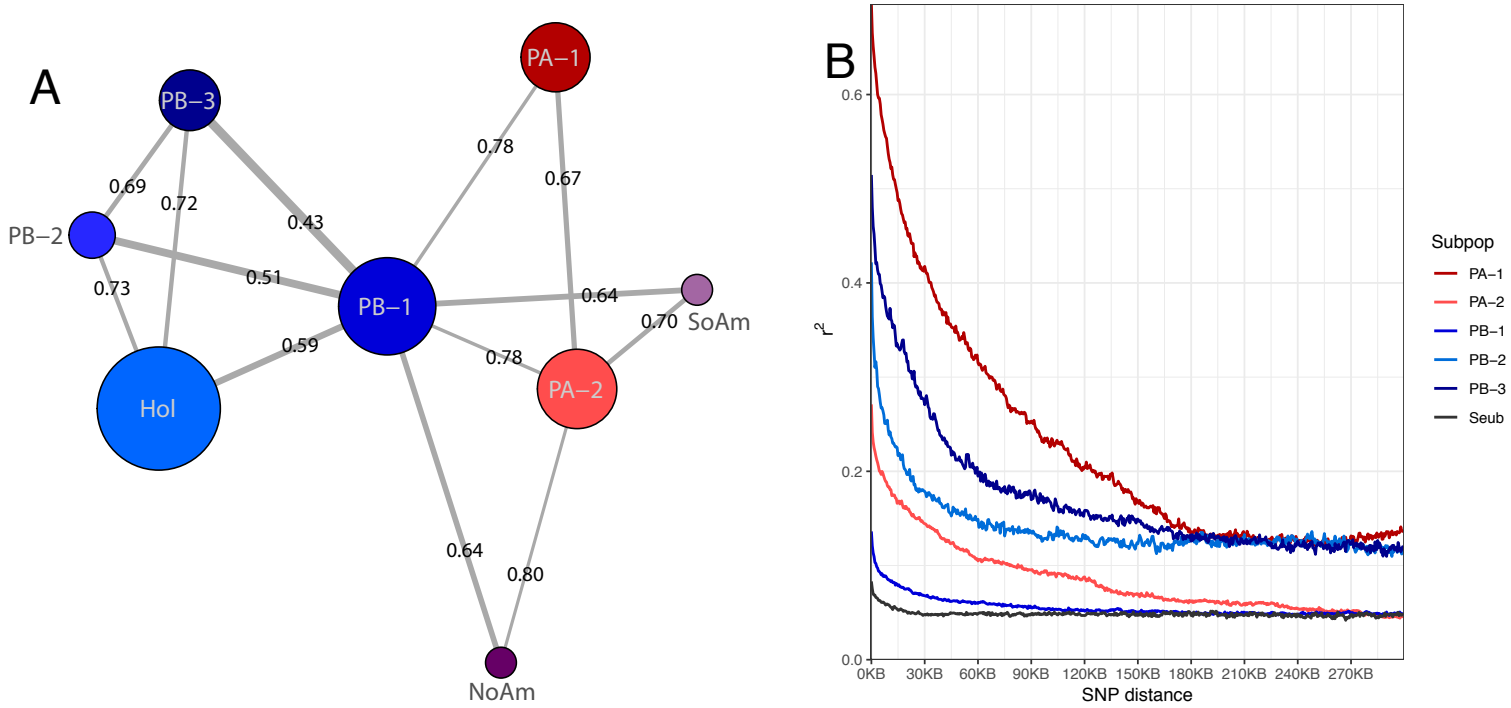

Figure 4

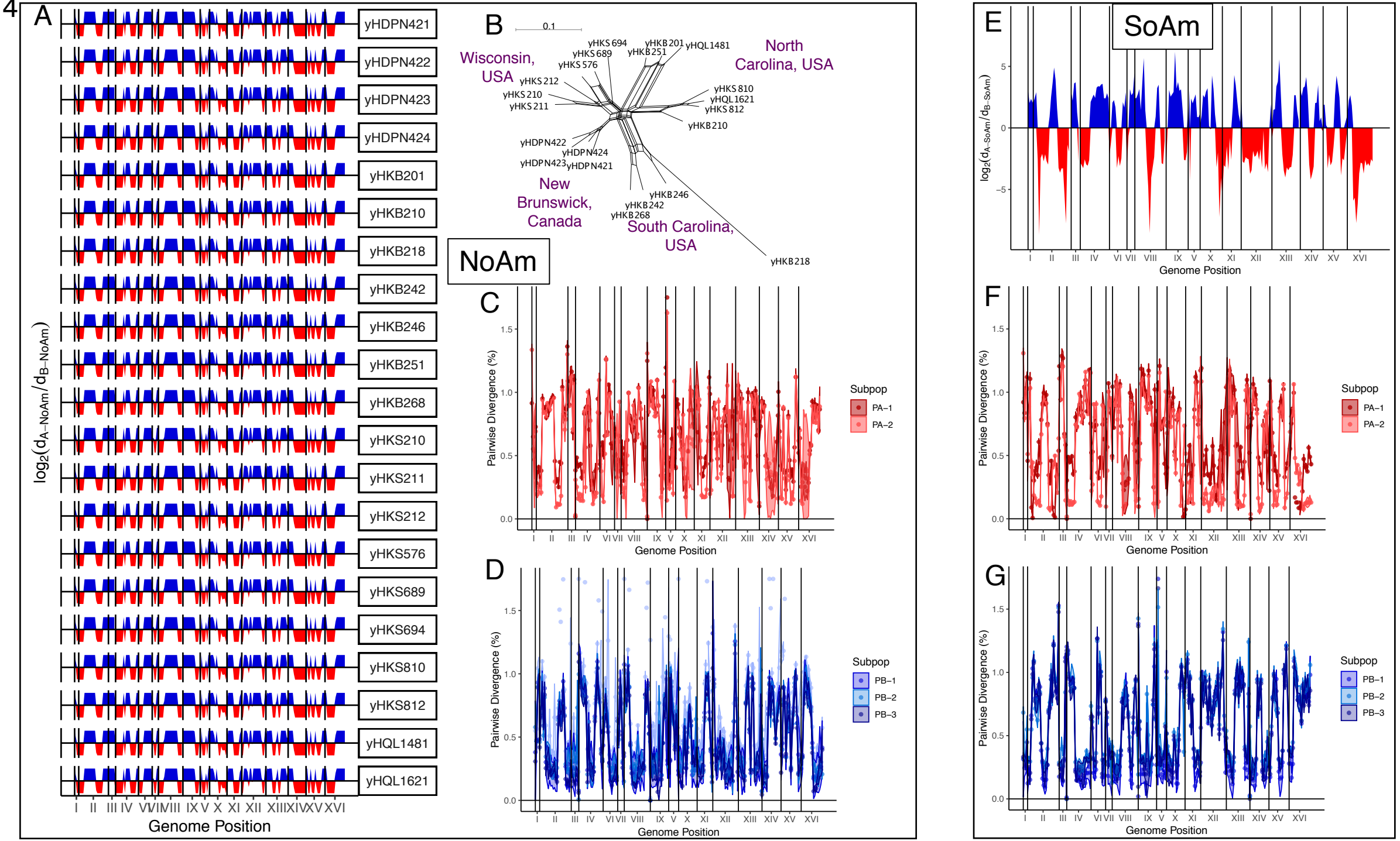
A
yHDPN421
yHDPN422
yHDPN423
yHDPN424
yHKB201
yHKB210
yHKB218
yHKB242
yHKB246
yHKB251
yHKB268
yHKS210
yHKS211
yHKS212
yHKS576
yHKS689
yHKS694
yHKS810
yHKS812
yHQL1481
yHQL1621
I II III IV V VI VII VIII IX V X XI XII XIII XIV XV XVI
Genome Position
log2(dA–NoAm/dB–NoAm)
B
0.1
Wisconsin, USA
North Carolina, USA
New Brunswick, Canada
South Carolina, USA
yHKS 694
yHKB 201
yHQL1481
yHKS 689
yHKB 251
yHKS 576
yHKS 212
yHKS 210
yHKS 211
yHKS 810
yHQL1621
yHKS 812
yHKB 210
yHDP N422
yHDP N424
yHDP N423
yHDP N421
yHKB 246
yHKB 242
yHKB 268
yHKB 218
NoAm
C
Pairwise Divergence (%)
Genome Position
Subpop
PA–1
PA–2
D
Pairwise Divergence (%)
Genome Position
Subpop
PB–1
PB–2
PB–3
E
SoAm
log2(dA–SoAm/dB–SoAm)
Genome Position
F
Pairwise Divergence (%)
Genome Position
Subpop
PA–1
PA–2
G
Pairwise Divergence (%)
Genome Position
Subpop
PB–1
PB–2
PB–3

Figure 5

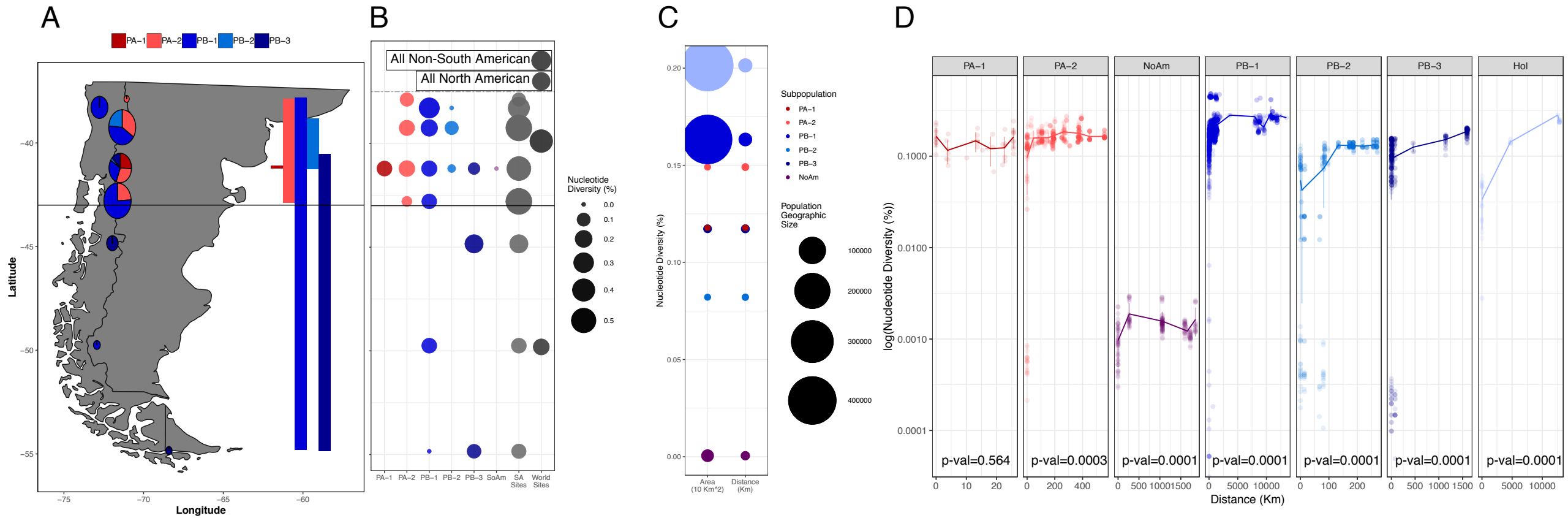
A
PA–1
PA–2
PB–1
PB–2
PB–3
Latitude
Longitude
B
All Non-South American
All North American
PA–1
PA–2
PB–1
PB–2
PB–3
SoAm
SA Sites
World Sites
Nucleotide Diversity (%)
C
Nucleotide Diversity (%)
Area (10 Km^2)
Distance (Km)
Subpopulation
Population Geographic Size
D
log(Nucleotide Diversity (%))
Distance (Km)
p-val=0.564
p-val=0.0003
p-val=0.0001
p-val=0.0001
p-val=0.0001
p-val=0.0001
p-val=0.0001

Figure 6

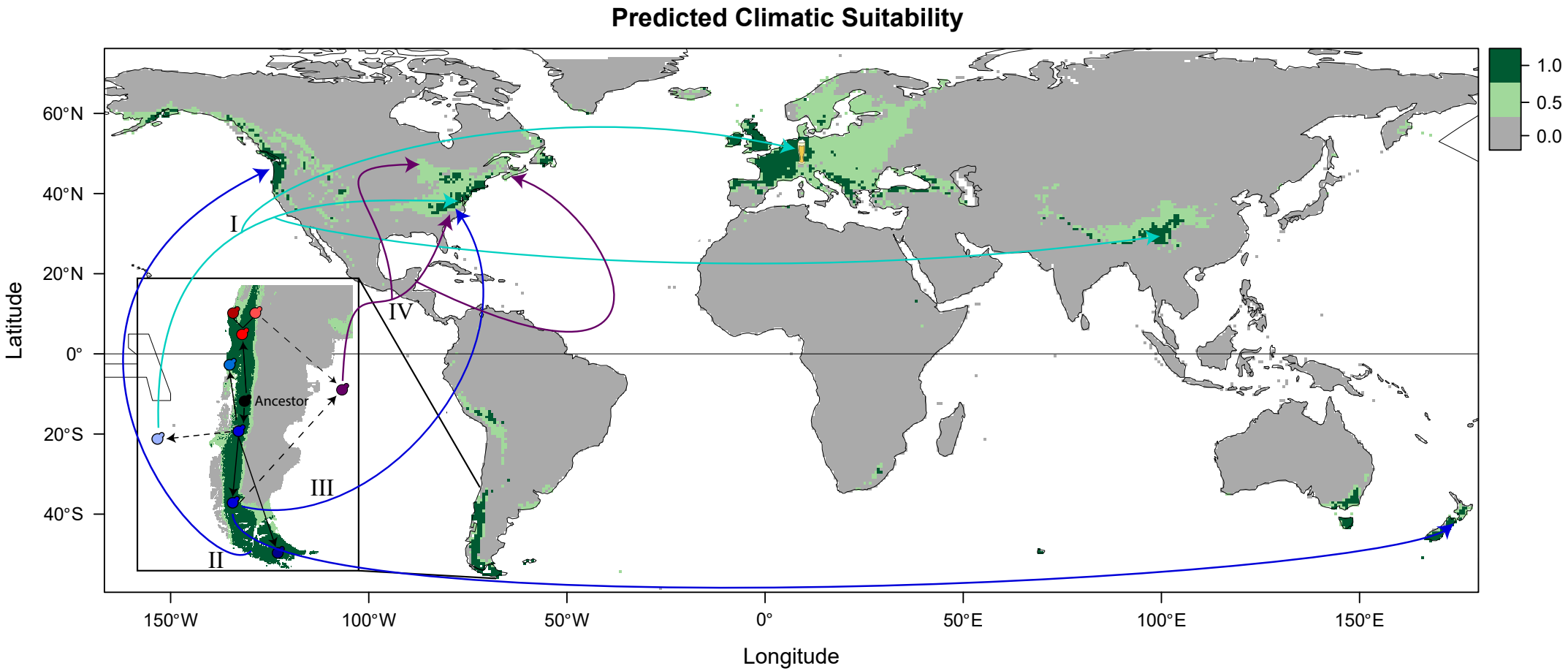
Predicted Climatic Suitability
1.0
0.5
0.0
60°N
40°N
20°N
0°
20°S
40°S
Latitude
150°W
100°W
50°W
0°
50°E
100°E
150°E
Longitude
Ancestor
I
II
III
IV

Figure S1

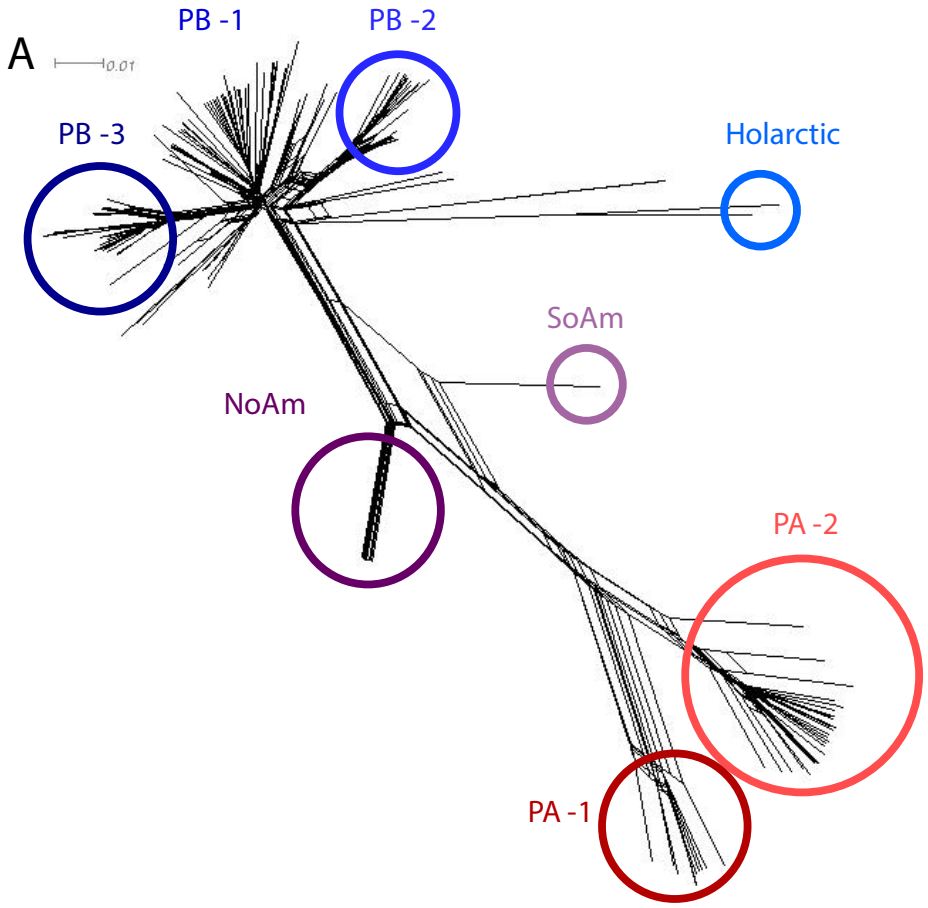
A
0.01
PB -1
PB -2
PB -3
Holarctic
SoAm
NoAm
PA -2
PA -1

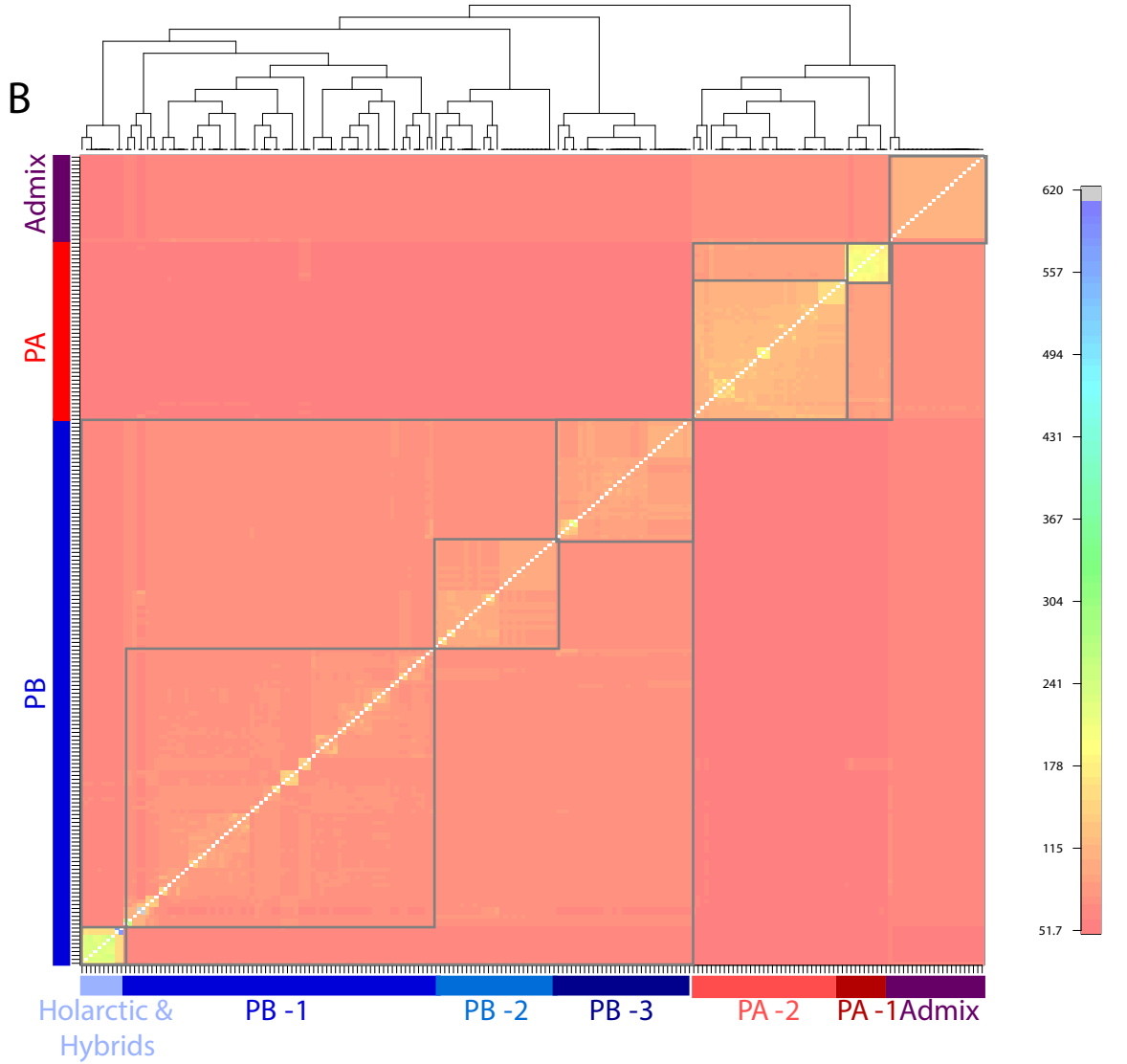
B
Admix
PA
PB
620
557
494
431
367
304
241
178
115
51.7
Holarctic & Hybrids
PB -1
PB -2
PB -3
PA -2
PA -1
Admix

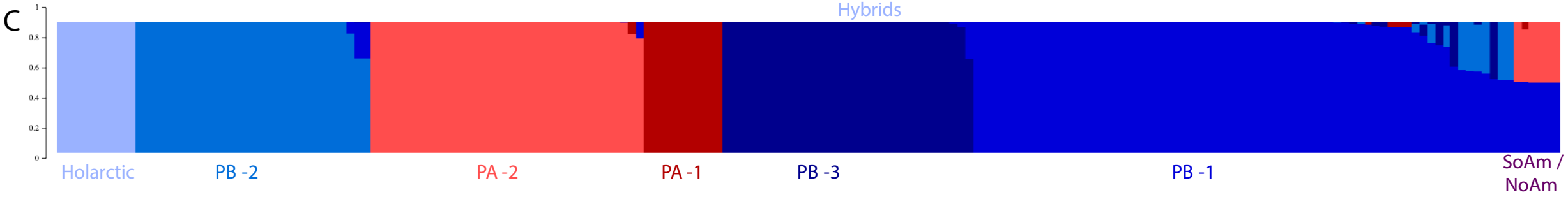
C
1
0.8
0.6
0.4
0.2
0
Holarctic
PB -2
PA -2
PA -1
PB -3
PB -1
SoAm / NoAm

Figure S2

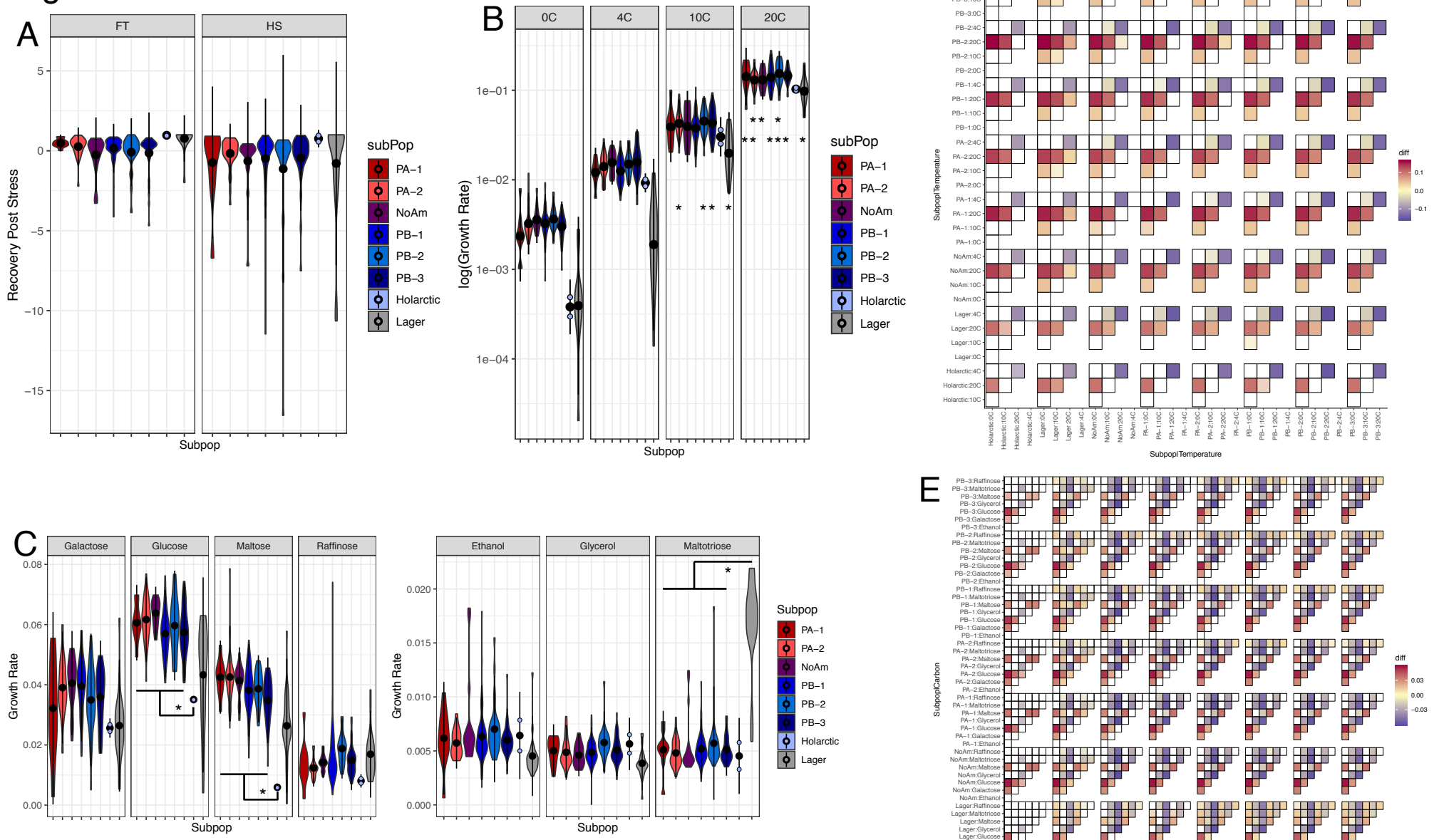
A
FT
HS
Recovery Post Stress
Subpop
subPop
PA–1
PA–2
NoAm
PB–1
PB–2
PB–3
Holarctic
Lager
B
0C
4C
10C
20C
log(Growth Rate)
Subpop
subPop
C
Galactose
Glucose
Maltose
Raffinose
Ethanol
Glycerol
Maltotriose
Growth Rate
Subpop
Subpop
D
SubpopTemperature
diff
E
SubpopCarbon
diff

Figure S3

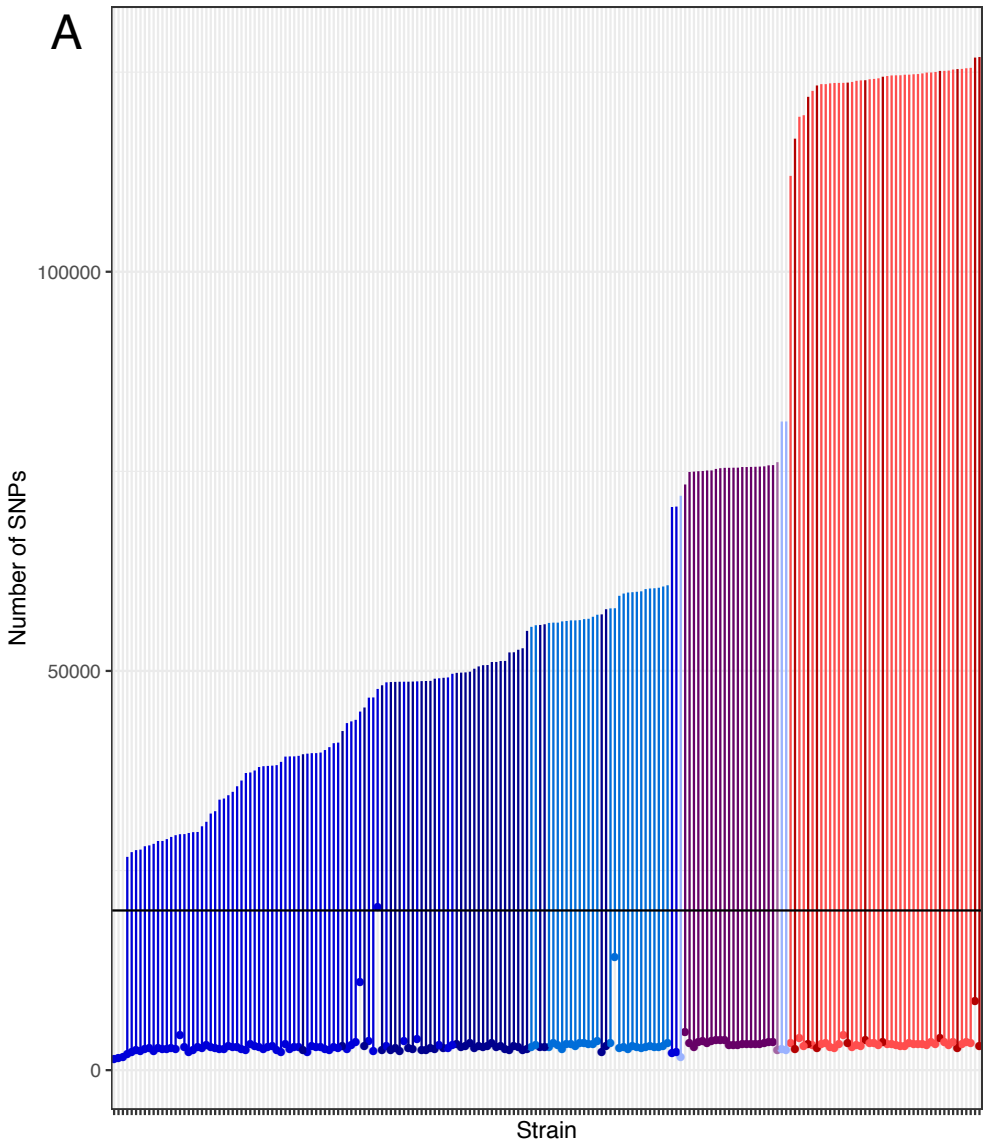
A
100000
50000
0
Number of SNPs
Strain
Subpop
Holarctic
NoAm
PA–1
PA–2
PB–1
PB–2
PB–3
SoAm

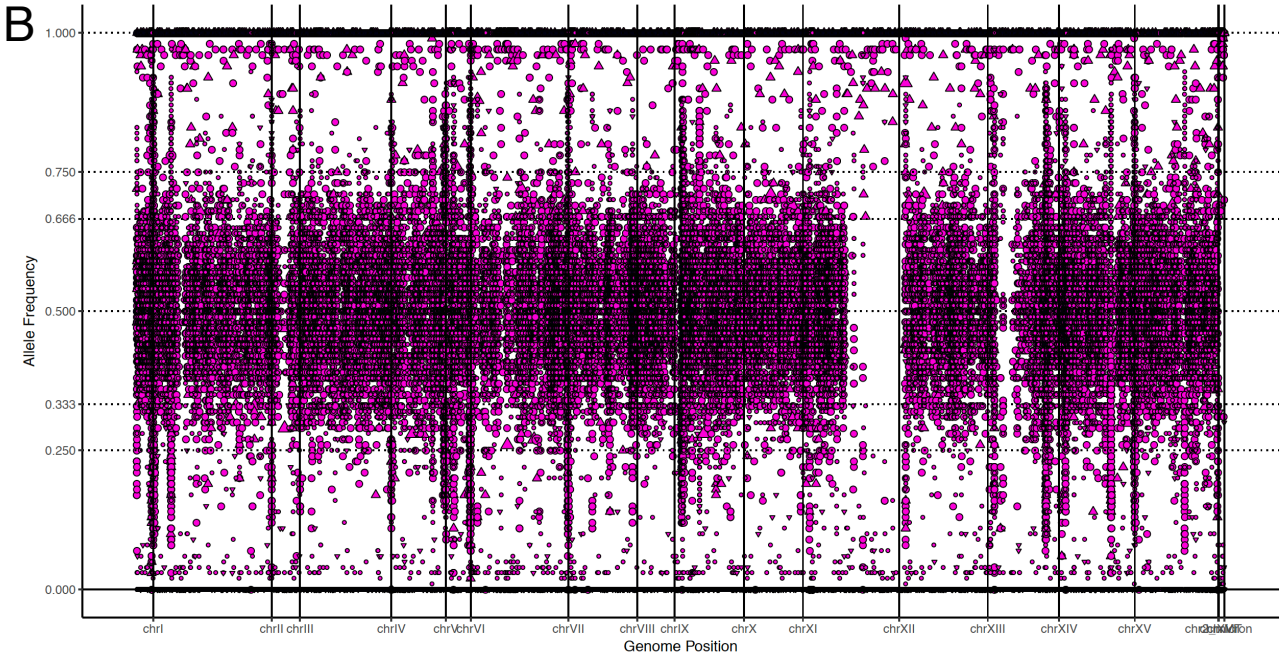
B
1.000
0.750
0.666
0.500
0.333
0.250
0.000
Allele Frequency
chrI
chrII
chrIII
chrIV
chrV
chrVI
chrVII
chrVIII
chrIX
chrX
chrXI
chrXII
chrXIII
chrXIV
chrXV
Genome Position
Allele type
del
in
SNP

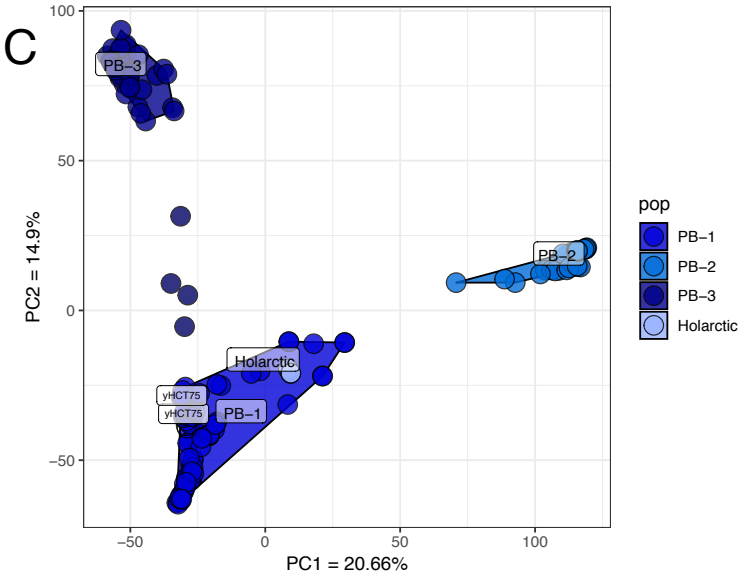
C
100
50
0
−50
PC2 = 14.9%
−50
0
50
100
PC1 = 20.66%
PB–3
PB–2
Holarctic
yHCT75
yHCT75
PB–1
pop
PB–1
PB–2
PB–3
Holarctic

Figure S4

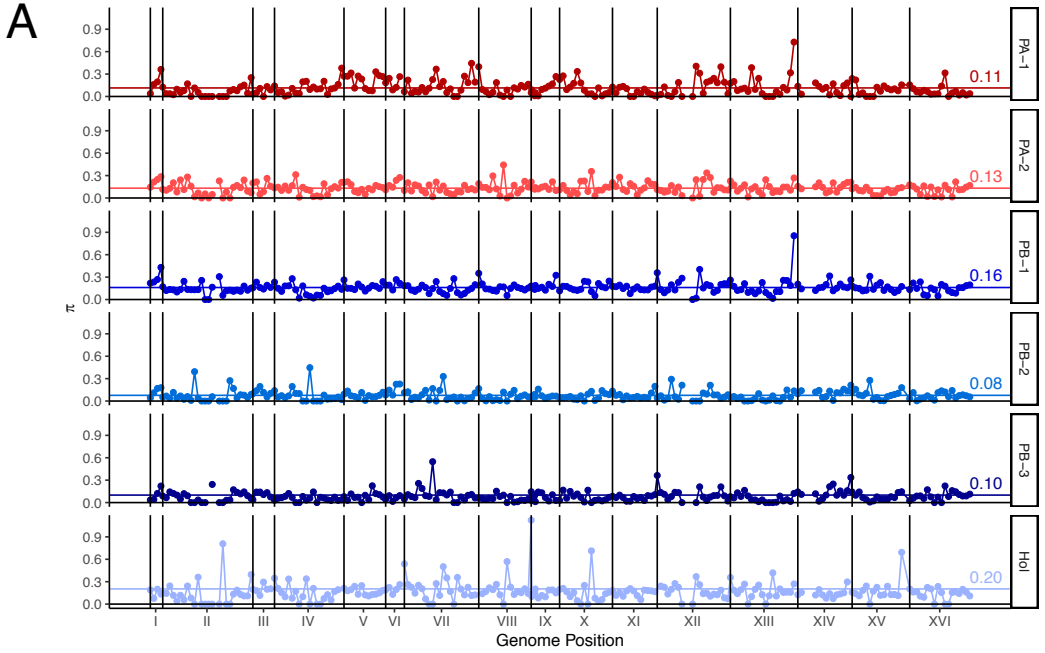
A
π
PA–1
PA–2
PB–1
PB–2
PB–3
Hol
0.11
0.13
0.16
0.08
0.10
0.20
Genome Position

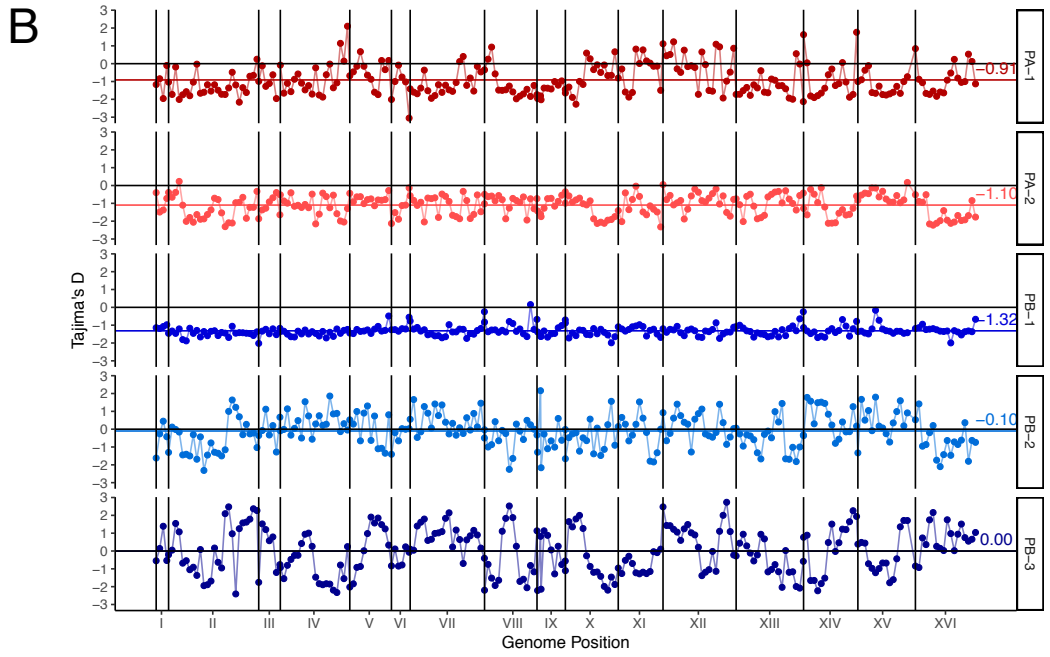
B
Tajima's D
PA–1
PA–2
PB–1
PB–2
PB–3
−0.91
−1.10
−1.32
−0.10
0.00
Genome Position

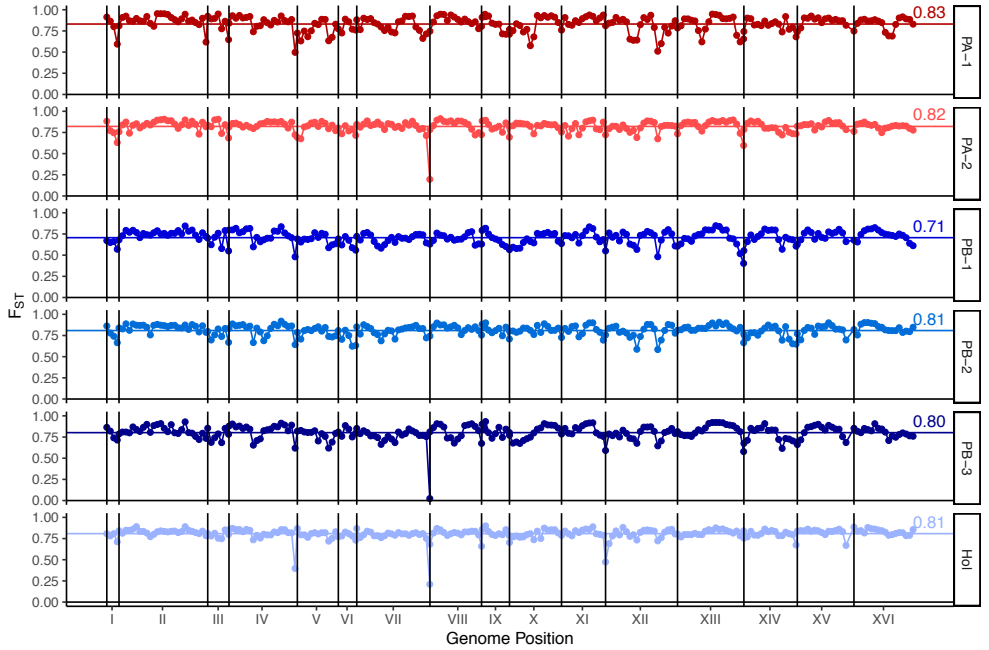
C
FST
PA–1
PA–2
PB–1
PB–2
PB–3
Hol
0.83
0.82
0.71
0.81
0.80
0.81
Genome Position

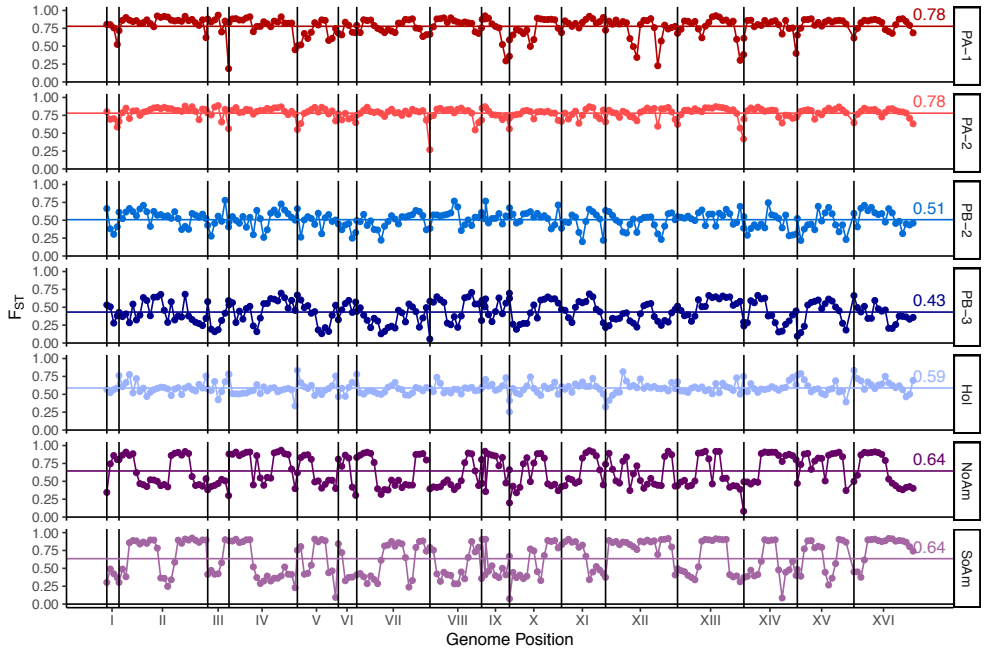
D
FST
PA–1
PA–2
PB–2
PB–3
Hol
NoAm
SoAm
0.78
0.78
0.51
0.43
0.59
0.64
0.64
Genome Position

Figure S5

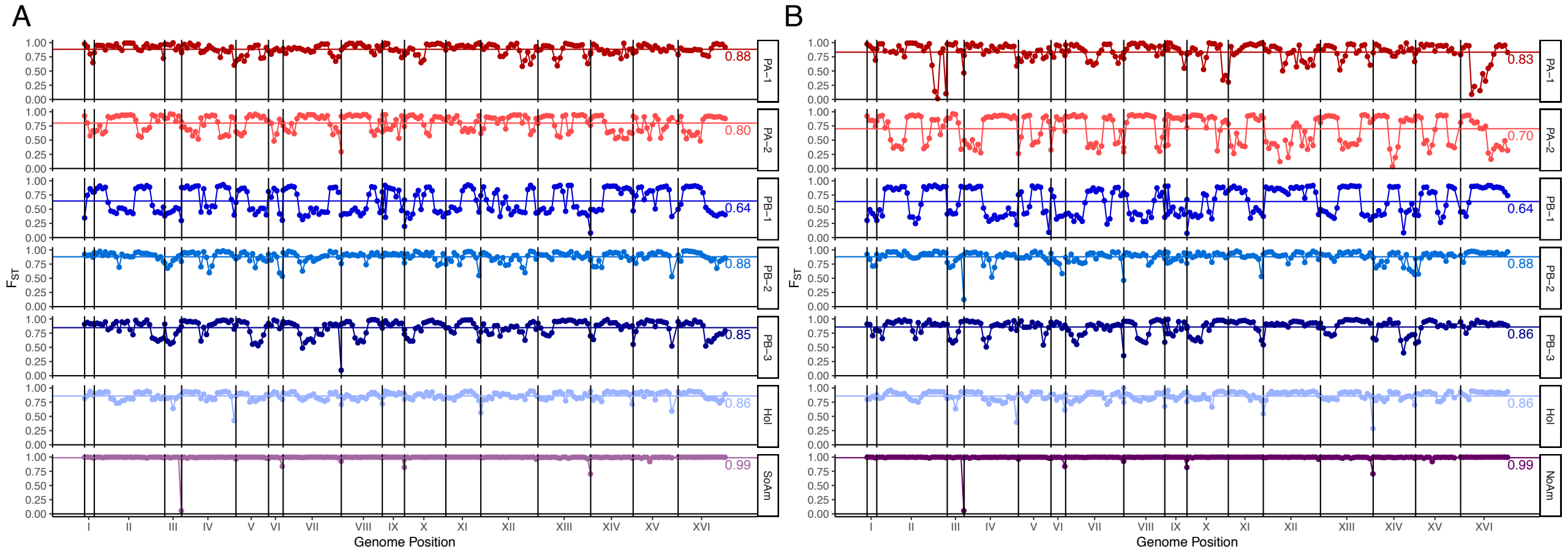
A
B
F_{ST}
1.00
0.75
0.50
0.25
0.00
PA–1
PA–2
PB–1
PB–2
PB–3
HoI
SoAm
NoAm
0.88
0.80
0.64
0.88
0.85
0.86
0.99
0.83
0.70
0.64
0.88
0.86
0.86
0.99
I
II
III
IV
V
VI
VII
VIII
IX
X
XI
XII
XIII
XIV
XV
XVI
Genome Position

Figure S6

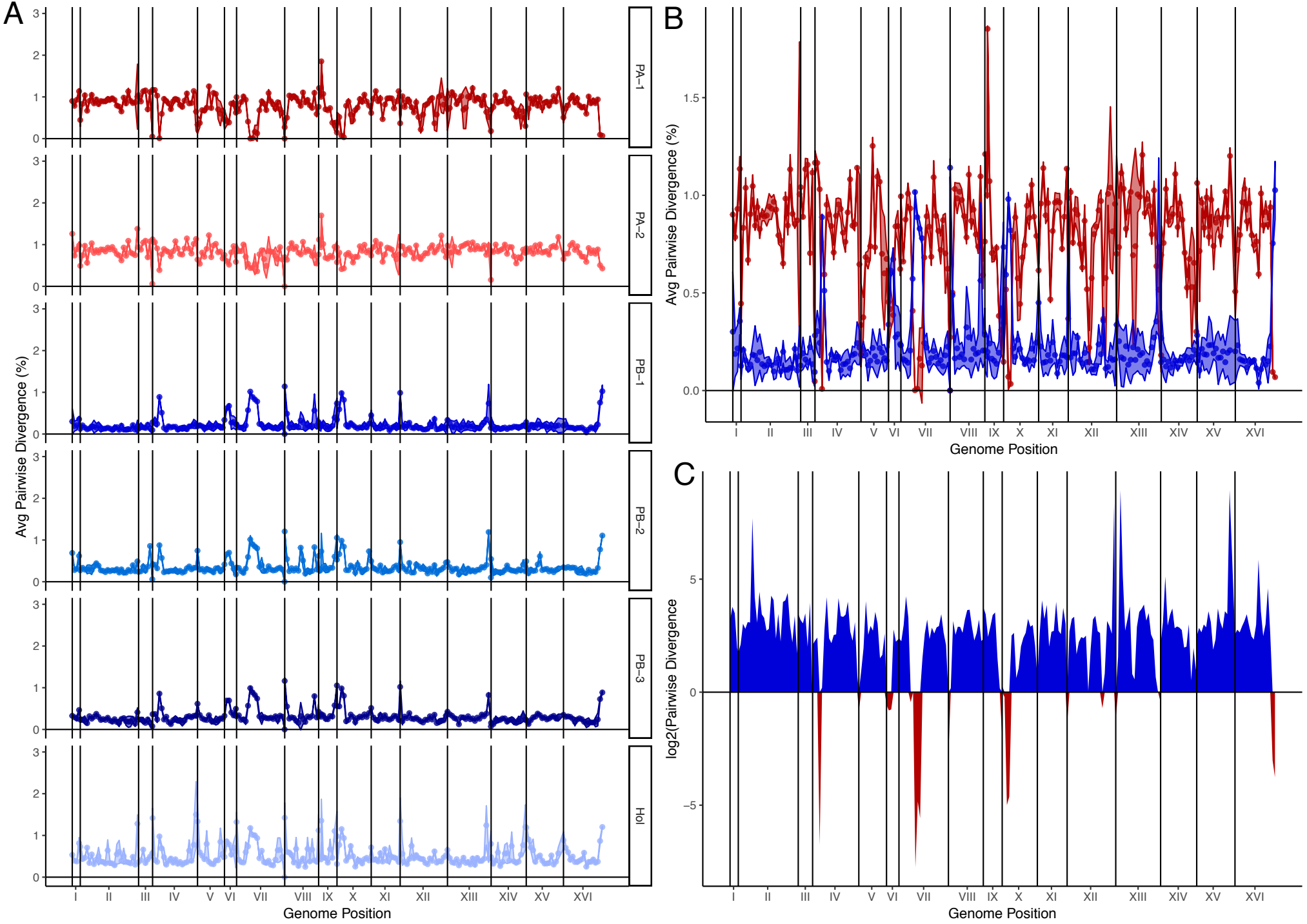
A
B
C
PA–1
PA–2
PB–1
PB–2
PB–3
Hol
Avg Pairwise Divergence (%)
log2(Pairwise Divergence
Genome Position
I
II
III
IV
V
VI
VII
VIII
IX
X
XI
XII
XIII
XIV
XV
XVI

Figure S7

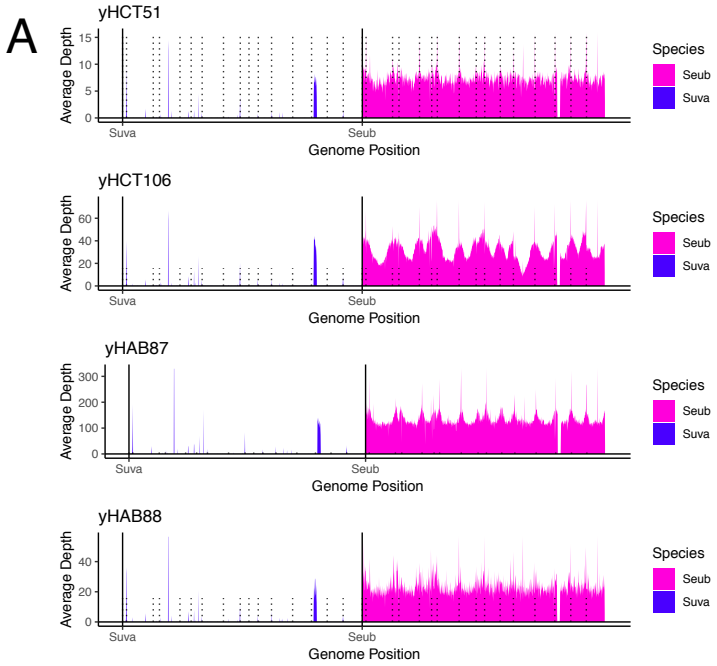
A
yHCT51
yHCT106
yHAB87
yHAB88
Average Depth
Genome Position
Suva
Seub
Species
Seub
Suva

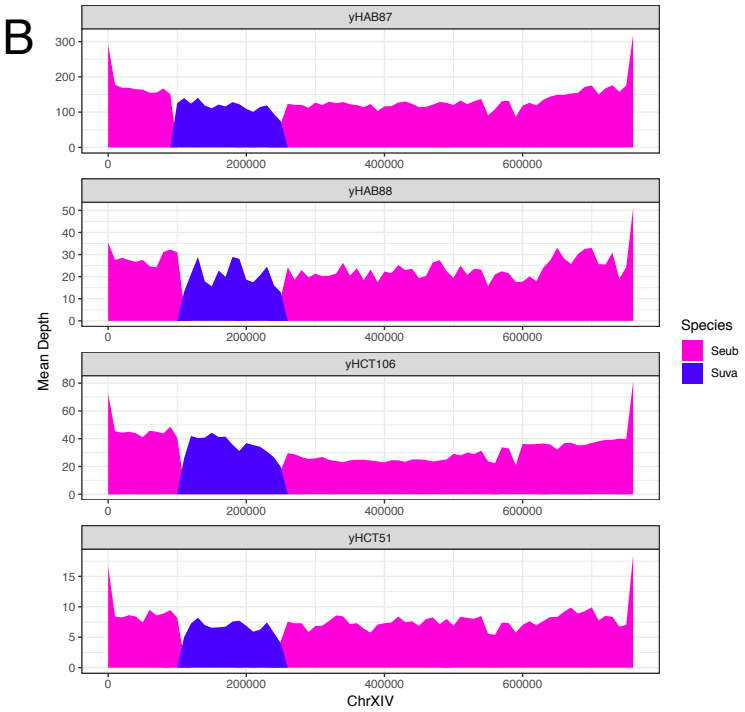
B
yHAB87
yHAB88
yHCT106
yHCT51
Mean Depth
ChrXIV
Species
Seub
Suva

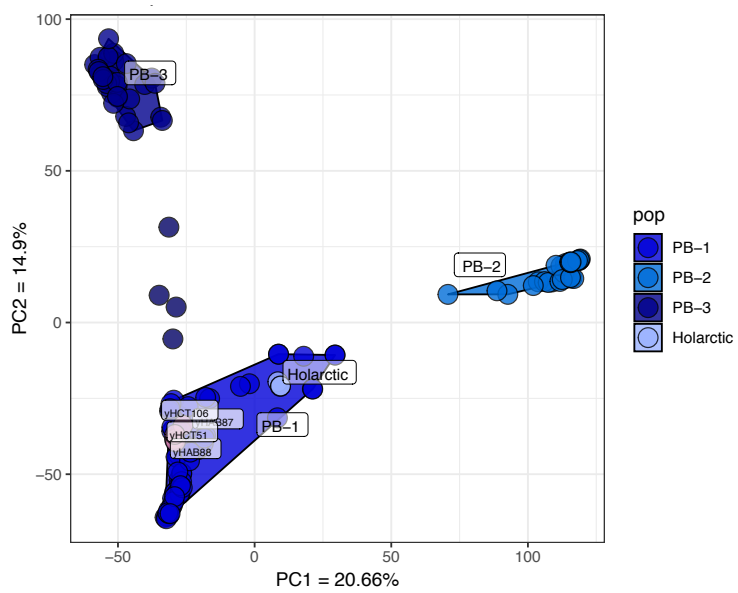
C
PB–3
PB–2
Holarctic
PB–1
yHCT106
yHAB87
yHCT51
yHAB88
PC2 = 14.9%
PC1 = 20.66%
pop
PB–1
PB–2
PB–3
Holarctic

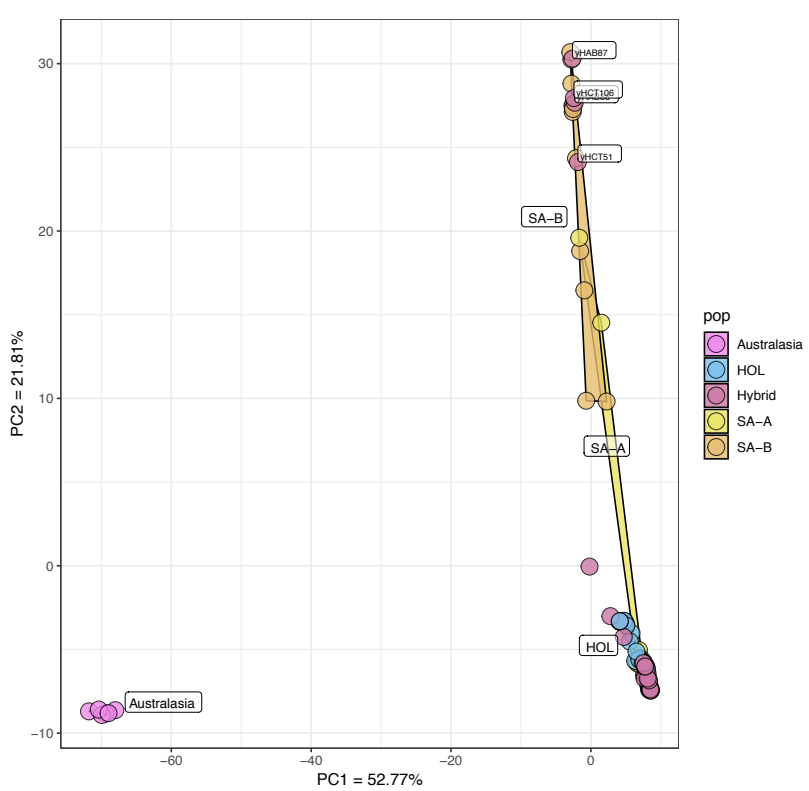
D
yHAB87
yHCT106
yHCT51
SA–B
SA–A
HOL
Australasia
PC2 = 21.81%
PC1 = 52.77%
pop
Australasia
HOL
Hybrid
SA–A
SA–B

Figure S8

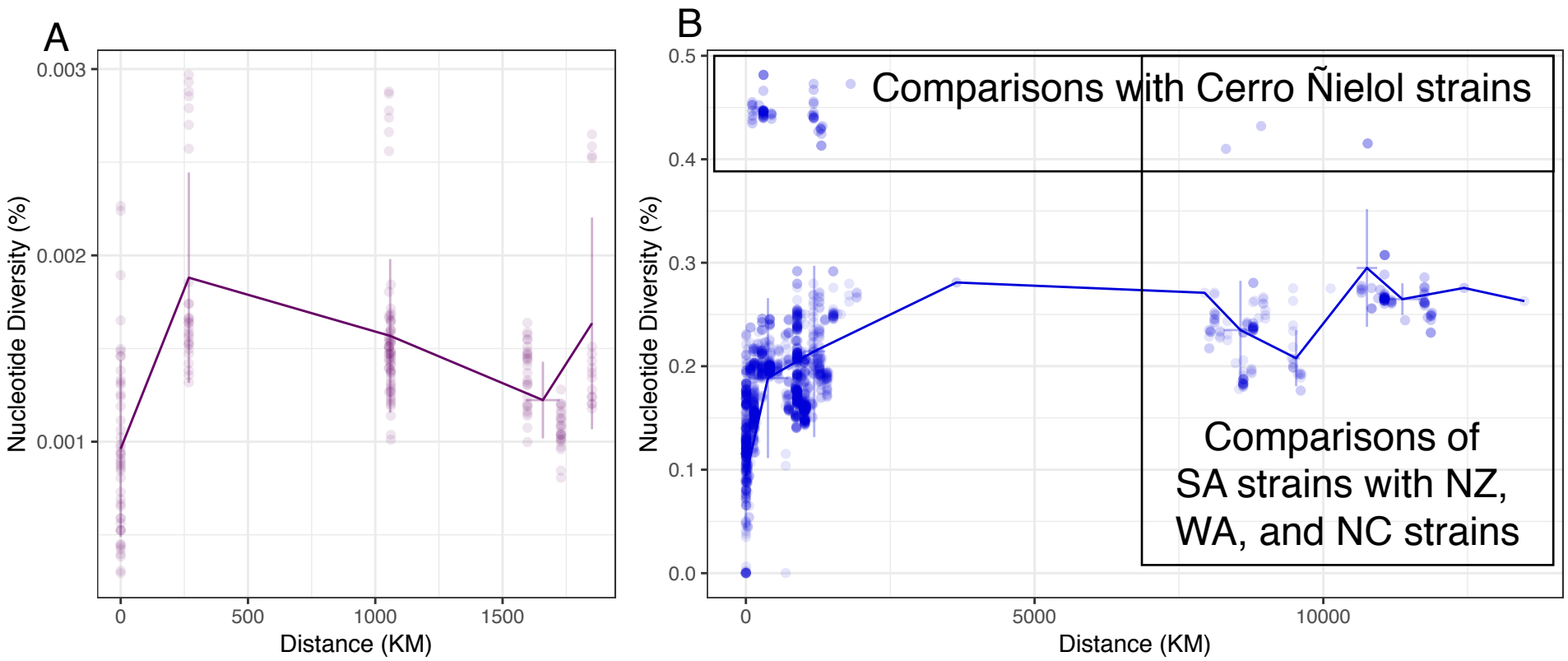
A
0.003
0.002
0.001
Nucleotide Diversity (%)
0
500
1000
1500
Distance (KM)
B
0.5
0.4
0.3
0.2
0.1
0.0
Nucleotide Diversity (%)
Comparisons with Cerro Ñielol strains
Comparisons of
SA strains with NZ,
WA, and NC strains
0
5000
10000
Distance (KM)

Figure S9

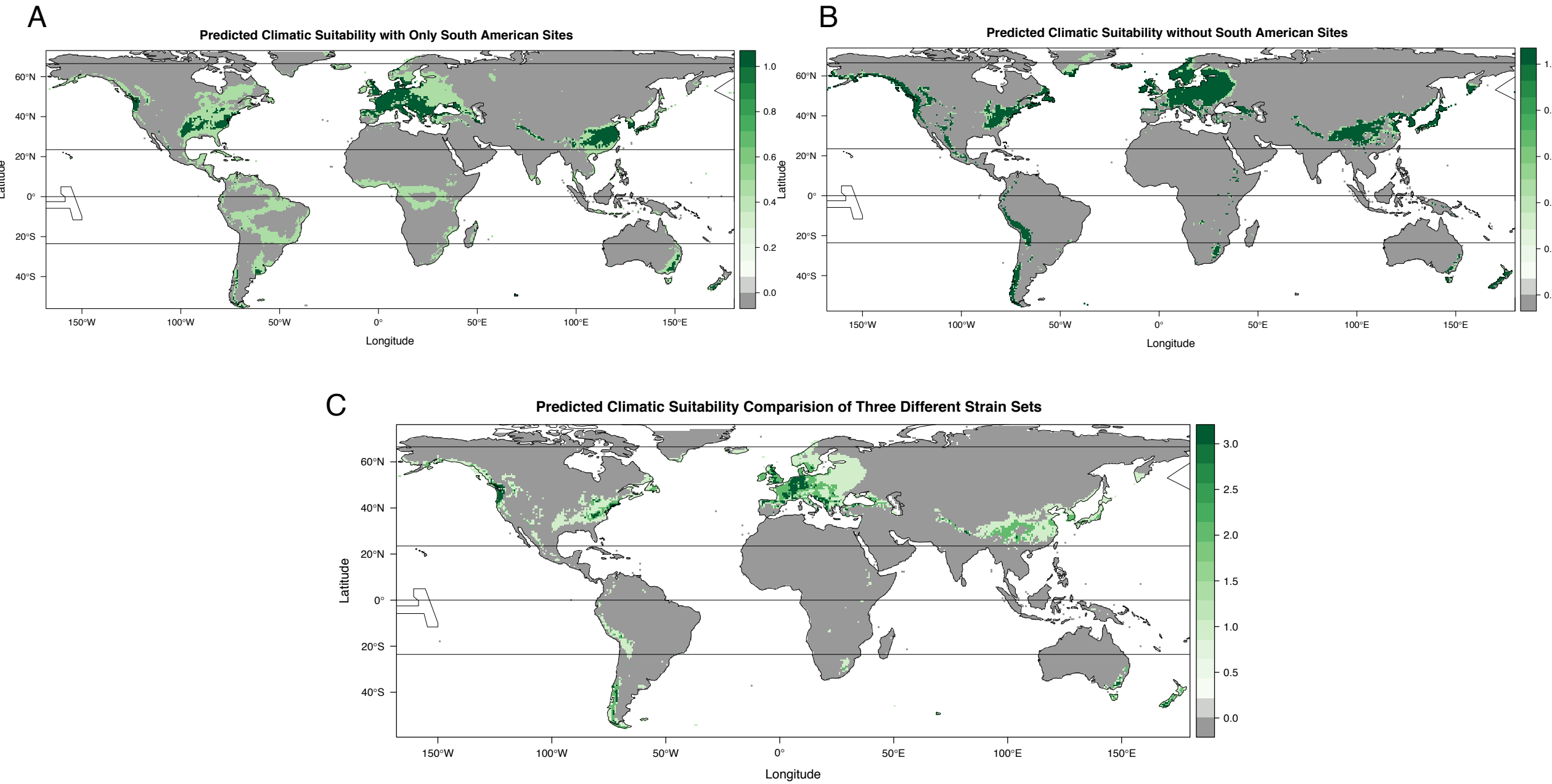
A
Predicted Climatic Suitability with Only South American Sites
B
Predicted Climatic Suitability without South American Sites
C
Predicted Climatic Suitability Comparision of Three Different Strain Sets
Latitude
Longitude
60°N
40°N
20°N
0°
20°S
40°S
150°W
100°W
50°W
0°
50°E
100°E
150°E
1.0
0.8
0.6
0.4
0.2
0.0
3.0
2.5
2.0
1.5
1.0
0.5
0.0